

## **Azimuth Modulation of C- and Ku-band Radar Backscatter Over Antarctica From ASCAT and SeaWinds Data**

9 Feb 2011

David Long  
Brigham Young University

Strong, steady winds give rise to coherent structuring of snow in Antarctica. Sastrugi and the Antarctic Megadunes are particular examples of this, but such structuring extends below the surface via wind-driven preferential deposition and inter-annual layering. Coupled with local topography, these effects introduce a dependency of radar backscatter on the azimuth direction of the observations. This is termed 'azimuth modulation'. Microwave azimuth modulation was first explored by Long and Drinkwater (2000) for passive microwave measurements and the Ku-band NASA Scatterometer (NSCAT) and the C-band ERS-1/2 scatterometers. These initial studies revealed that the azimuth dependence of the normalized radar cross section ( $\sigma_0$ ) can be quite large and is closely correlated with the wind direction. In fact, they showed that the dominant wind direction could be derived with surprising accuracy from the azimuth dependency of the scatterometer-observed backscatter. The analysis has been extended to Greenland (Ashcraft and Long, 2005; 2006), and can even be applied in the Sahara desert (Stephen and Long, 2005)!

While many land regions exhibit a negligible amount of azimuth modulation (e.g. tropical rainforest), ignoring the azimuth dependency of the backscatter is ill-advised in others regions such as Antarctica and Greenland. The observed azimuth modulation of radar backscatter has profound implications for other radar sensors as well, including synthetic aperture radar (SAR) systems. When multiple observations or images are compared, if the azimuth angles of the observations are not identical, there may be a difference in the observed surface  $\sigma_0$ . This could easily be misinterpreted as a change in the surface, when it really is merely due to the differences in the  $\sigma_0$  values at different azimuth angles. This may be particularly important when studying long-term changes in the ice sheet.

To help ameliorate this concern, we have generated a data product derived from scatterometer observations that exploits the multi-azimuth observation capability of the scatterometer to estimate the azimuth modulation of the ice sheet. This data set can be used to compute an estimate of the azimuth modulation based on the differences in the azimuth angles of the sensor observation. This value can be used to "correct" the observation to eliminate (or at least minimize) the potential for falsely ascribing an observed change in  $\sigma_0$  that is due to azimuth modulation, to some other source, e.g. increased melting or accumulation.

While very well calibrated, scatterometers have much coarser resolution than SARs. To better enable our product to support this correction process for SARs, we use resolution enhancement techniques to estimate the spatial variation of the azimuth modulation at the finest possible spatial scale [see (Long and Drinkwater, 2000)]. Effectively, an AVE-type algorithm is employed in computing the azimuth modulation characteristics on a fine-scale (at least for a scatterometer) grid with a resolution of 4.45 km in a polar stereographic projection.

The particular azimuth sampling characteristics of NSCAT and ERS-1/2 limited the analysis in Long and Drinkwater [2007] to second order dependence on the azimuth angle. However, the rotating pencil-beam SeaWinds scatterometer and the dual-side, three-beam nature of the ESA Advanced Scatterometer (ASCAT) permit extension of the analysis to fourth order. This better models the

observed azimuth modulation in most areas of Antarctica. Data from these two sensors are used in the following.

In general, the azimuth modulation is a function of incidence angle (Long and Drinkwater, 2000); however, here we consider a simplified form that is not dependent on incidence angle. At a given location the sigma-0 (in dB) is written as,

$$\sigma^o = a + b(\theta - 40) + \varepsilon + \sigma_{az}^o(\varphi) \quad (1)$$

where  $a$  is the normalized radar cross-section normalized to a 40 deg incidence angle,  $b$  is the slope of sigma-0 versus incidence angle,  $\theta$  is incidence angle in deg,  $\varepsilon$  is the residual error, and the final term is the azimuth modulation as a function of the azimuth angle  $\varphi$  of the microwave look direction relative to north. This definition of azimuth angle is used for convenience since the local slope can be folded into the azimuth modulation and so not be explicitly needed in computing the geometry (Long and Drinkwater, 2000). Since QuikSCAT observations are limited to a single incidence angle for each polarization, for QuikSCAT  $b$  is set to zero and the  $a$  coefficient corresponds to the sigma-0 at the nominal incidence angle for the particular polarization of interest.

For this paper the fourth-order azimuth modulation term is expressed as

$$\sigma_{az}^o(\varphi) = \sum_{k=1}^4 m_k \cos(\varphi - \phi_k) \quad (2)$$

where  $m_k$  and  $\phi_k$  are the azimuth modulation parameters estimated from the scatterometer data for the particular location. The  $m_k$  parameter is the magnitude of the  $k^{\text{th}}$  order modulation while  $\phi_k$  is the phase angle parameter. For historical reasons and to fit within the standard BYU .sir file naming scheme, each azimuth modulation parameter is given single letter name as indicated in Table 1

*Table 1. Azimuth modulation coefficients and .sir file designation separated by a colon.*

Index	Magnitude	Phase
1	$m_1 : q$	$\phi_1 : r$
2	$m_2 : s$	$\phi_2 : t$
3	$m_3 : Q$	$\phi_3 : R$
4	$m_4 : S$	$\phi_4 : T$

We have found that the Ku-band azimuth modulation parameters do not exhibit significant seasonal change in areas that do not experience melt, and have minimal variation over the mission. A similar conclusion appears valid for C-band (work underway). For areas that experience seasonal melt, the azimuth modulation tends to be very small. Thus, for now we have provided a single, time-constant set of parameters over Antarctica in the form of an image array. We believe that is adequate for a first-order correction for the effects of azimuth modulation. A more comprehensive analysis will be included in a paper currently in preparation. We consider azimuth modulation coefficients estimated from the C-band ASCAT scatterometer and the Ku-band QuikSCAT scatterometer.

The prototype azimuth modulation correction data set is derived from 30 days of data from mid winter. For ASCAT we used JD 182-212, 2010, while for QuikSCAT we used JD 200-229, 2007. (The precise dates are arbitrarily chosen and will be reconciled in the paper in preparation. Images of model parameters for each sensor data set are provided in the Appendix. To generate estimates for each azimuth modulation coefficient, the  $a$  and  $b$  coefficients are first separately estimated for each pixel using the AVE algorithm. The other coefficients are then estimated using a least-squares algorithm. To

reduce noise, the images are median filtered. (A much more detailed description of the derivation is contained in the paper in preparation.)

## ASCAT

The C-band ASCAT employs six antenna beams that collect data over a roughly 20-65 deg incidence angle range on each side of the nadir track (ASCAT, 2009). Combining multiple passes, each pixel location in the 4.45 km grid is observed multiple times at different azimuth and incidence angles. Unfortunately, the region near the pole is observed by only one side of the spacecraft and thus has significantly few azimuth angle observations. This degrades the accuracy of the azimuth modulation parameters for latitudes south of approximately 78.25S falls off. North of this line, however, the estimates appear to be quite accurate. Evidence of this occurs in the spatial consistency of the estimates (see Fig. 4 and other examples in Appendix A).

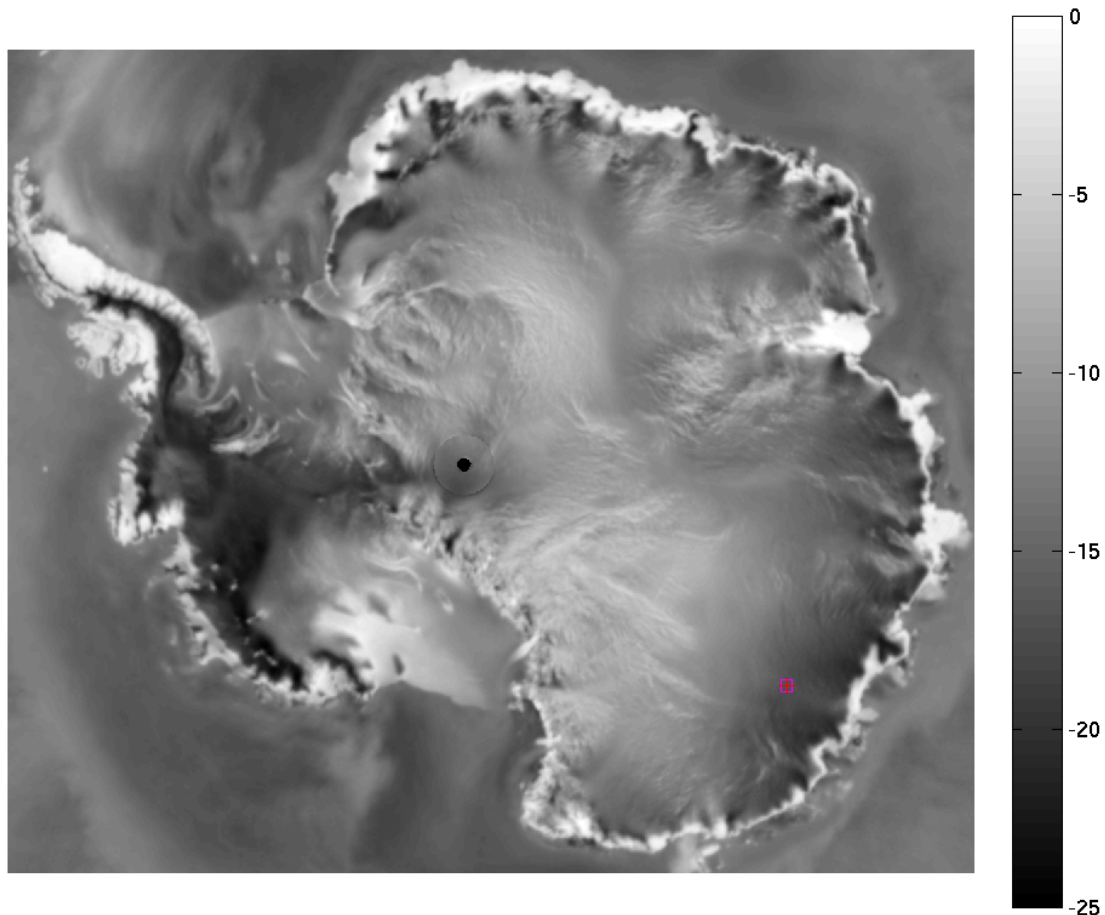


*Figure 1. ASCAT C-band sigma-0 in dB normalized to a 40 degree incidence angle (termed 'a'). The red box shows the study location.*

To illustrate the modulation and model fit, we extracted all raw ASCAT measurements whose centers fall within a box defined by [124.3E to 123.7E, 70.4S to 70.1 S]. Figure 1 shows the ASCAT  $a$  image and the location of this study area. Movement of sea ice during the imaging time period blurs the region outside of the continental area. Note that key topographical features are clearly evident, including the megadune region, summit, various ice shelves and mountains. The brightest regions are

those along the coast which experience annual melting, i.e. the percolation zone. In the percolation zone, buried ice glands increase the volume backscatter, resulting in a high backscatter.

The raw measurements extracted from the study region are incidence angle corrected using the reported incidence angle and the  $b$  coefficient computed using linear regression of the raw data. The incidence-angle corrected values are shown in Fig. 2 as cyan dots. The particular distribution of azimuth angles varies with location, but this is a typical case. The fourth-order azimuth modulation computed from the coefficients stored in the data set for the pixel at the center of this location is shown as the solid line. Generally the curve fits the data well, though there some residual unmodelled error is apparent from -100 deg through about -50 deg. Note that magnitude of the azimuth modulation is  $\pm 6$  dB, distinctly non-negligible! The modulation curve by itself is shown in Fig. 3.

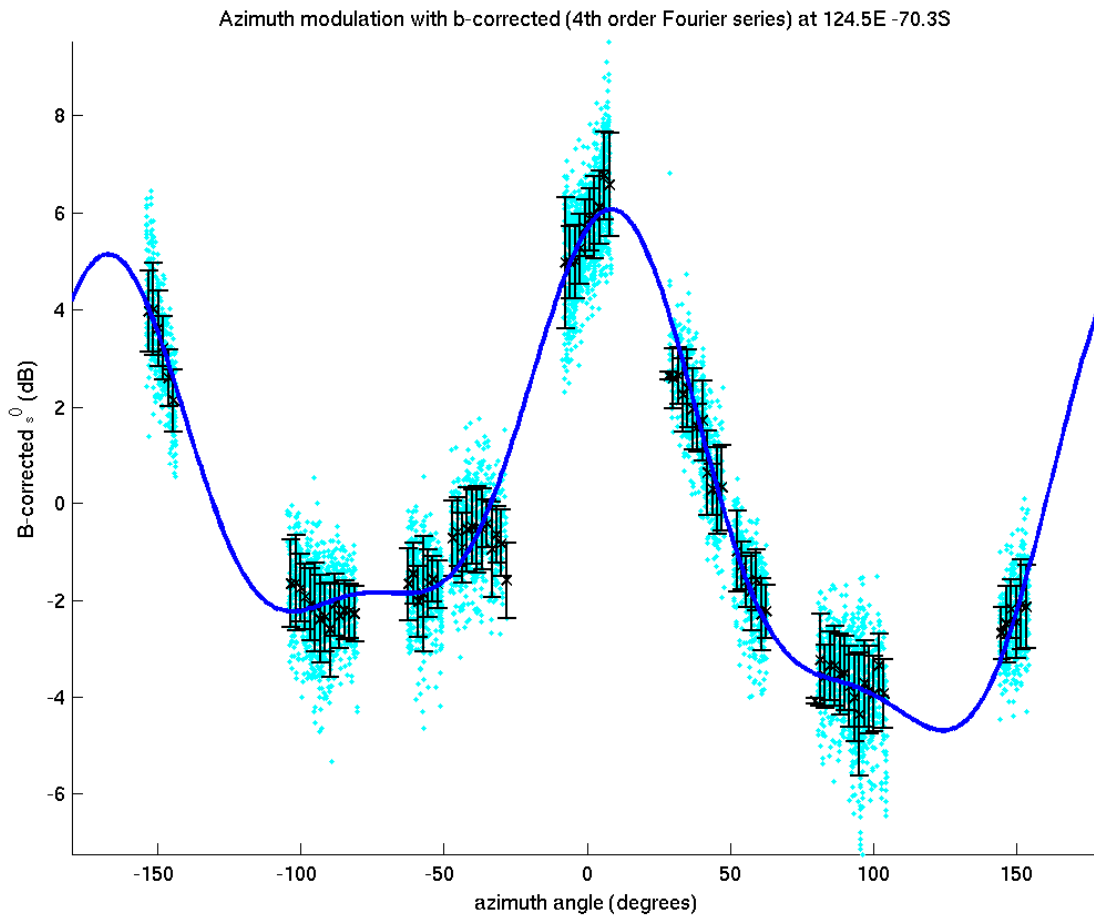


Figure 2. Scatterplot of incidence angle normalized ASCAT measurements plotted with respect to azimuth angle relative to north. These are binned in to small azimuth angle bins and the mean and standard deviation for each bin is computed. These are shown as error bars. The solid blue line shows the fourth-order Fourier series fit from the BYU ASCAT modulation files.

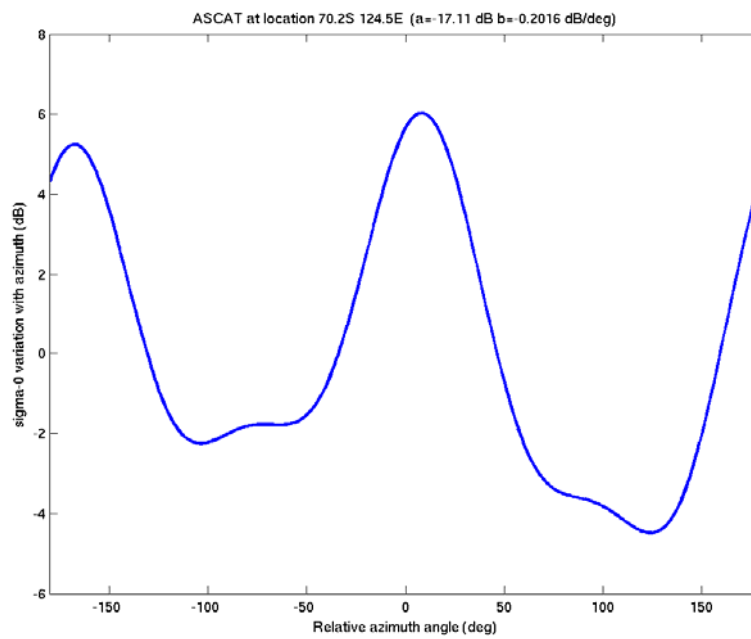


Figure 3. Plot of the fourth-order azimuth modulation of ASCAT C-band sigma-0 computed from the BYU ASCAT modulation files.

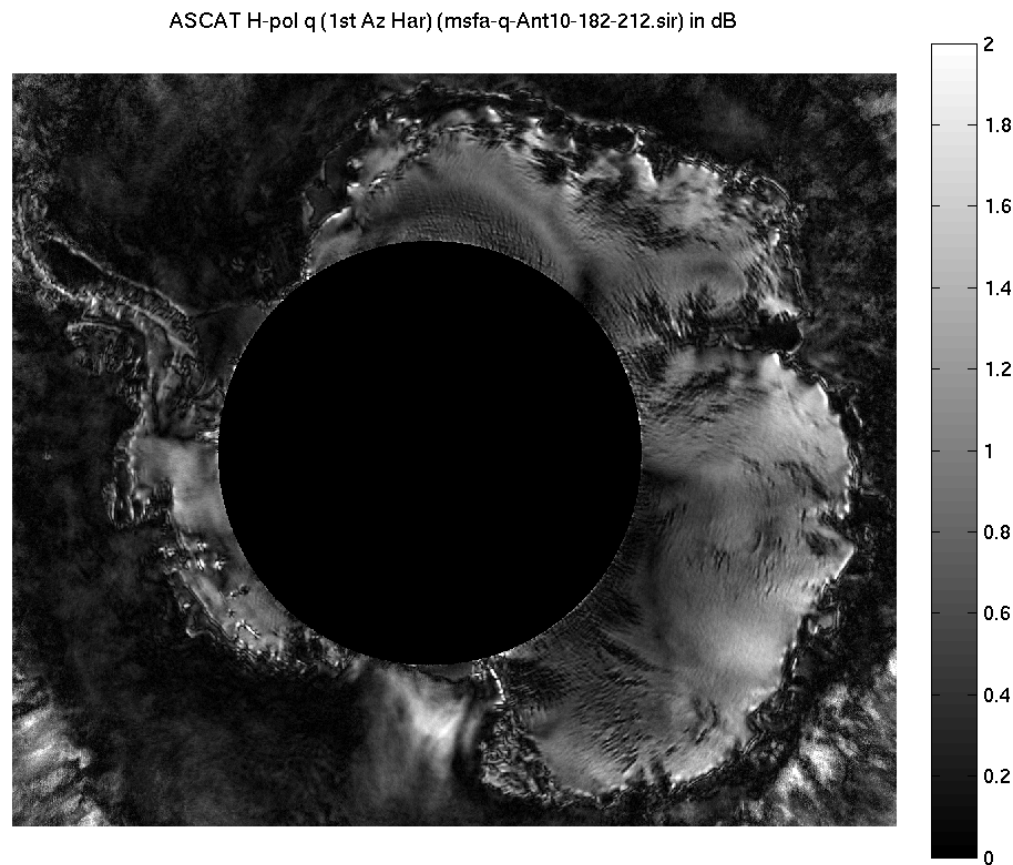


Figure 4. Image of the first-order magnitude azimuth modulation parameter with the “limited azimuth zone” indicated with a black circle. In this zone, the accuracy of the fourth-order model is reduced, see text.

## SeaWinds

The Ku-band SeaWinds scatterometer on QuikSCAT employs a dual-beam scanning pencil-beam antenna. Each beam operates at a different polarization and a constant incidence angle (46 deg for H-pol 54 deg for V-pol). The scanning geometry generates a wide diversity of azimuth angles at any given point on the surface, though the precise azimuth distribution depends on the latitude and can vary considerably. At low latitudes near the pole there is less azimuth diversity, leading to degraded performance in estimating the model coefficients. This is evident in the salt and pepper noise surrounding the pole in the images shown in Appendix B.

Figures 5 and 6 show the H-pol and V-pol Ku-band azimuth modulation for the study region previously described. Note that the QuikSCAT observations at this location span full azimuth angle range, and demonstrate that the azimuth modulation is, indeed, fourth order. Figure 7 compares the H-pol and V-pol fourth-order models, which are seen to be very similar. From this we conclude that the source of the modulation is not limited to a horizontal or vertical feature of the surface.

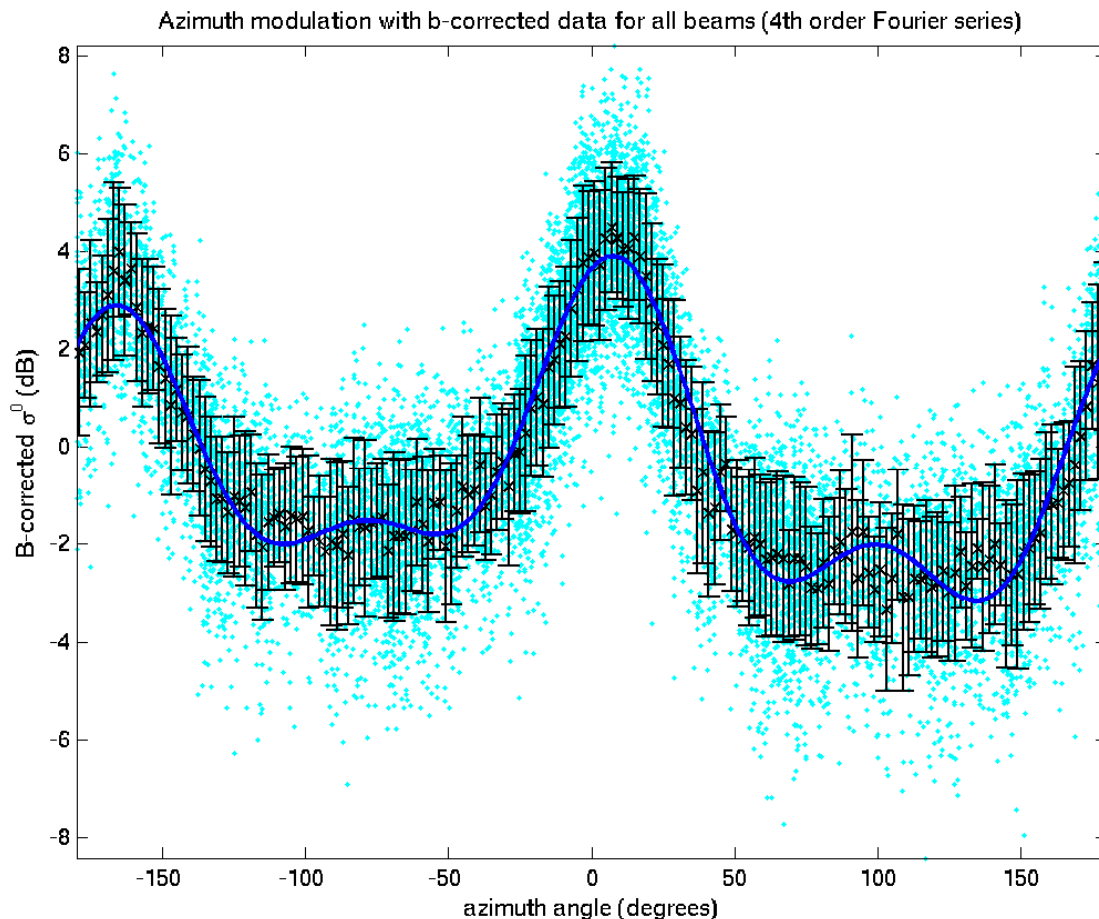


Figure 5. QuikSCAT H-pol sigma-0 measurements for the study region with the 4<sup>th</sup> order model fit.

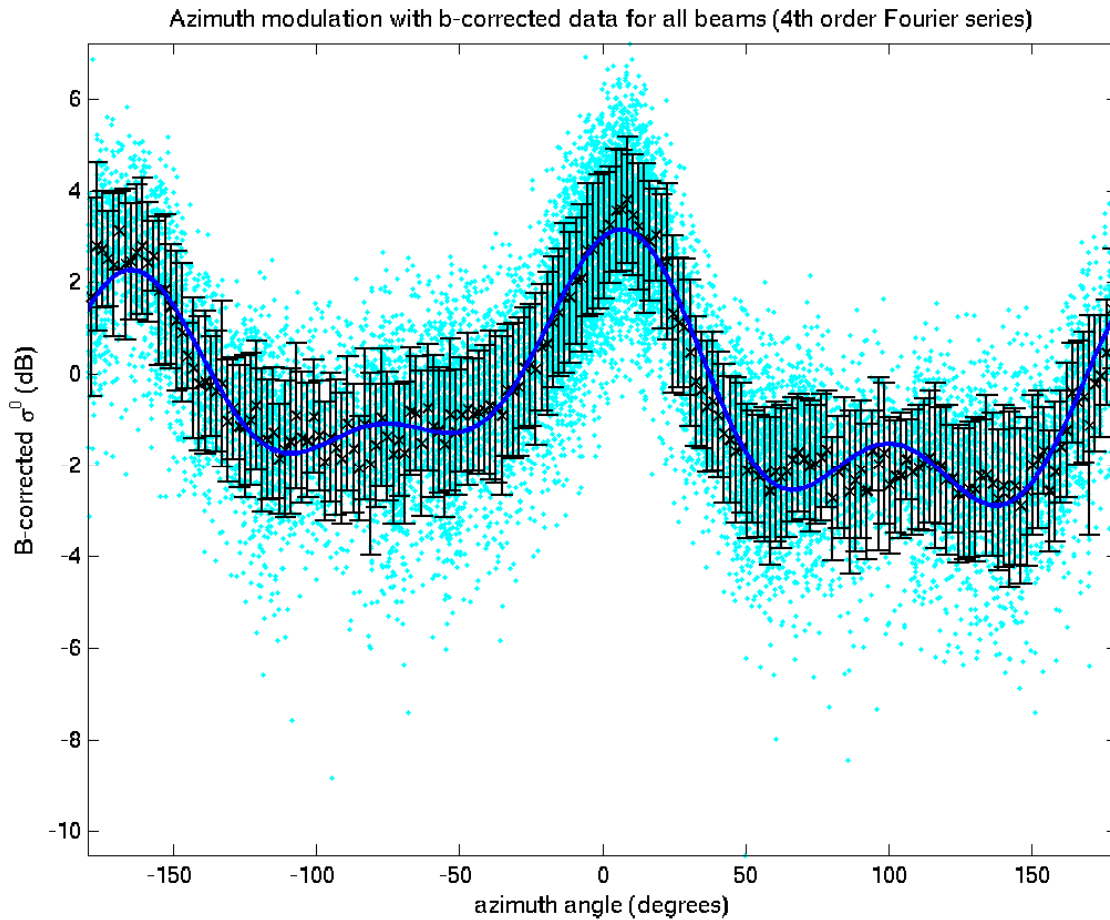


Figure 6. QuikSCAT V-pol sigma-0 measurements for the study region with the 4<sup>th</sup> order model fit.

In general, the observed azimuth modulation is similar for Ku-band and C-band as seen in Figs. 7 and 8. Note that the peaks and minimums occur at (essentially) the same azimuth angle, suggesting that they respond to the same physical phenomena.

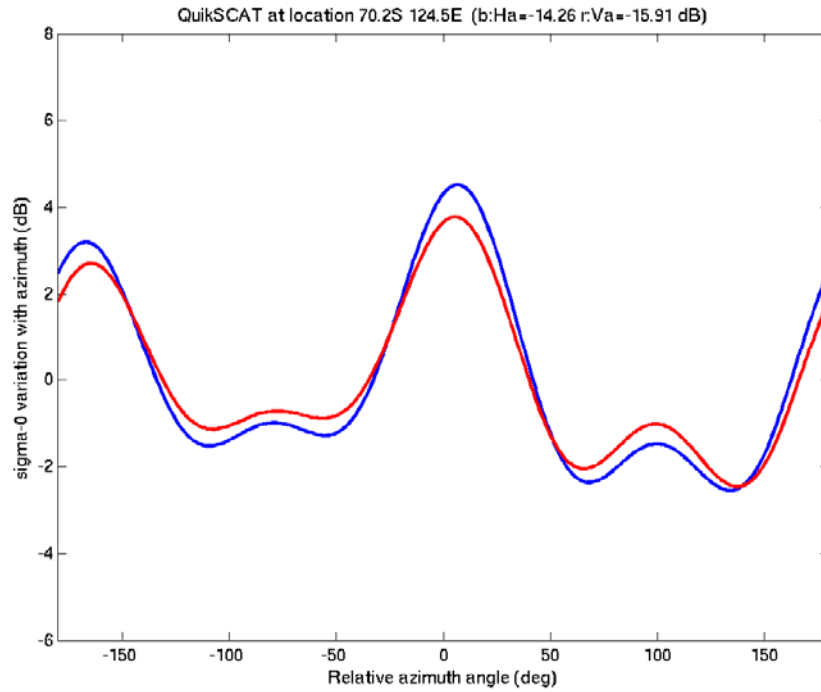


Figure 7. Comparison of QuikSCAT H-pol and V-pol azimuth modulation models for the study region.

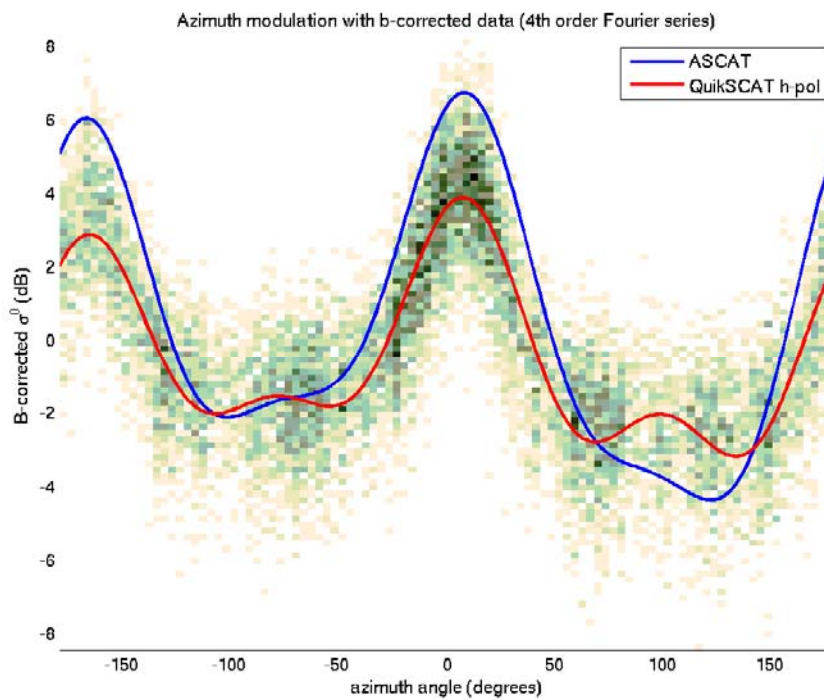


Figure 8. Comparison of QuikSCAT H-pol measurements and model to the ASCAT modulation model for the study region.



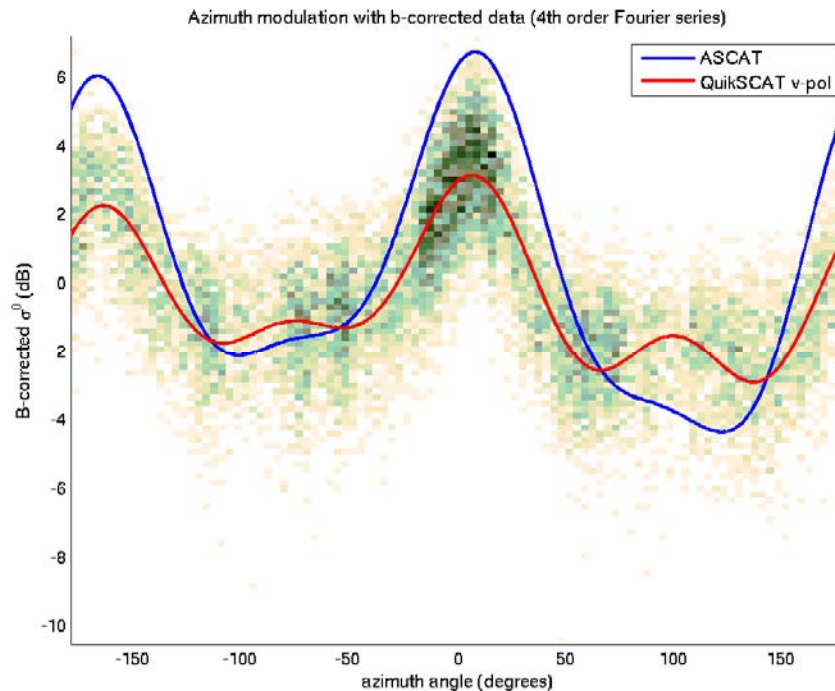


Figure 9. Comparison of QuikSCAT V-pol measurements and model to the ASCAT modulation model for the study region.

### Azimuth Modulation and Change Detection

In most areas of Antarctica, the azimuth modulation is sufficiently large that it should not be neglected when doing change detection. The proposed procedure to compensate for azimuth modulation is now described. For each location of interest (e.g. SAR image pixel), the azimuth angle relative to north of the microwave illumination is computed. The BYU azimuth modulation images are interpolated to the location and Eq. (2) computed. This yields an estimate of the azimuth modulation. When evaluating potential change between two images at different times and possible different azimuth angles, the difference in the azimuth modulation should be computed and included in the difference computation to estimate the change due to the only to the azimuth modulation. The residual difference is then the true change in backscatter.

I recognize that if the surface really did change (e.g. due to accumulation changes) between observation, that it is possible that azimuth modulation parameters may have changed as well. In such cases, further investigation of these locations may be warranted using a careful time series. However, to first-order based on our observations so far, changes in azimuth modulation over Antarctica appear to be small. For now, I recommend assuming the modulation is constant.

### Data Set Availability

I have posted beta versions of the data files containing the azimuth modulation parameters in (gzipped) BYU .SIR file format on our anonymous ftp site at <ftp://scp.byu.edu.edu/outgoing/data/ts/azmod/> in

separate subdirectories for each sensor. The main directory also includes a matlab script (studyarea.m) that illustrates how to read, plot, and compute the azimuth modulation. The subroutines this script calls are available in the software area on our ftp site. If you have any questions, let me know.

As previously noted, the ASCAT scatterometer observations extend from somewhat less than 20 deg incidence angle to nearly 65 deg. The ASCAT azimuth modulation data set is optimized at a 40 deg incidence angle, which is appropriate for scatterometer observations. Since SAR observations tend to be at much lower incidence angles, some error can be expected. It is possible, however, to derive coefficients optimized for use at a lower incidence angle, though this would be limited by the incidence angles of the available scatterometer observations. For QuikSCAT, the model has no incidence angle dependence. We previously derived second-order model coefficients with incidence angle dependence in Long and Drinkwater (2000).

## References

*ASCAT Users Manual*, EUMETSAT, Aug. 2009.

I.S. Ashcraft and D.G. Long, 2006. Relating Microwave Backscatter Azimuth Modulation to Surface Properties of the Greenland Ice Sheet, *Journal of Glaciology*, 52(177), 257-266.

I.S. Ashcraft and D.G. Long, 2005. Observation and Characterization of Radar Backscatter over Greenland, *IEEE Transactions on Geoscience and Remote Sensing*, 43(2), 237-246.

D.G. Long and M.R. Drinkwater, 2000. Azimuth Variation in Microwave Scatterometer and Radiometer Data Over Antarctica, *IEEE Transactions on Geoscience and Remote Sensing*, 38(4), 1857-1870.

H. Stephen and D.G. Long, 2005. Microwave Backscatter Modeling of Erg Surfaces in the Sahara Desert, *IEEE Transactions on Geoscience and Remote Sensing*, 43(2), 238-247.

*QuikSCAT Users Manual*, NASA/JPL, Jun. 2002.

## Appendix A

This appendix illustrates the various coefficients of our alpha-version of the ASCAT (C-band) 4<sup>th</sup> order azimuth modulation dataset. The various terms in the model are described in Eq. 1 in the main text.

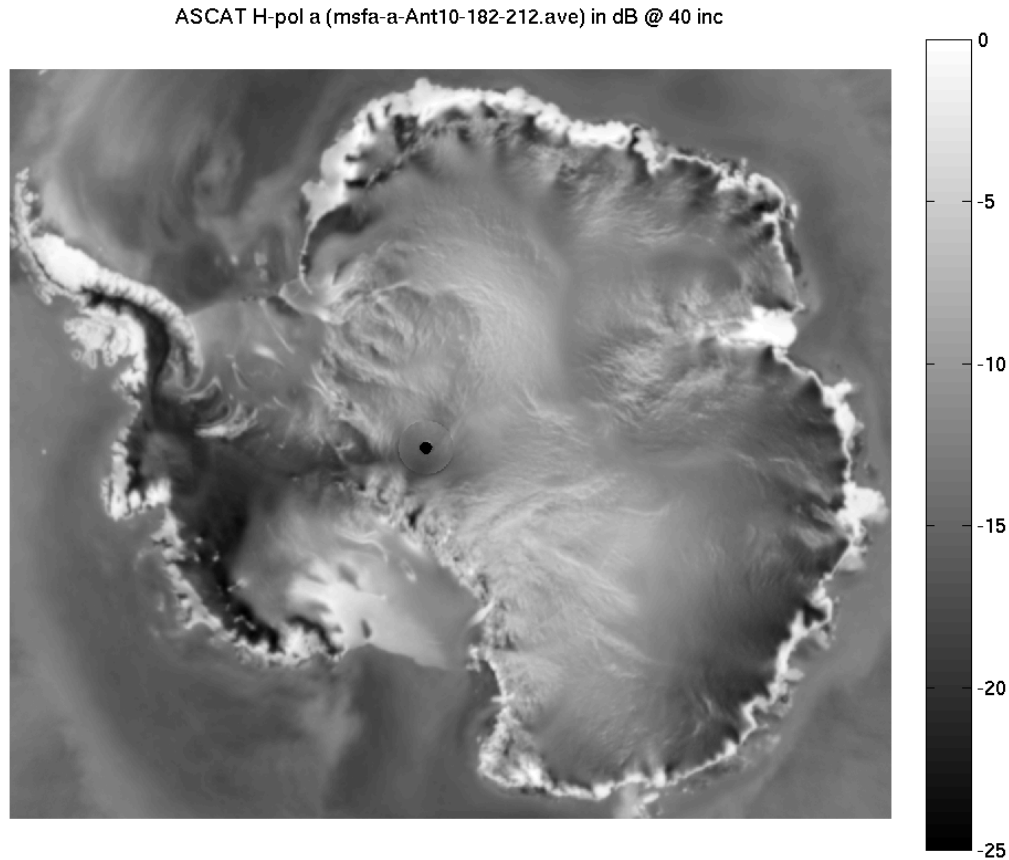


*Fig. A.1 ASCAT C-band sigma-0 in dB normalized to a 40 degree incidence angle (termed 'a'). Accuracy is reduced for latitudes less than 88.5S due to inadequate coverage and no estimate is possible for latitudes less than approximately 88.7S.*

ASCAT H-pol b (msfa-b-Ant10-182-212.ave) in dB/deg

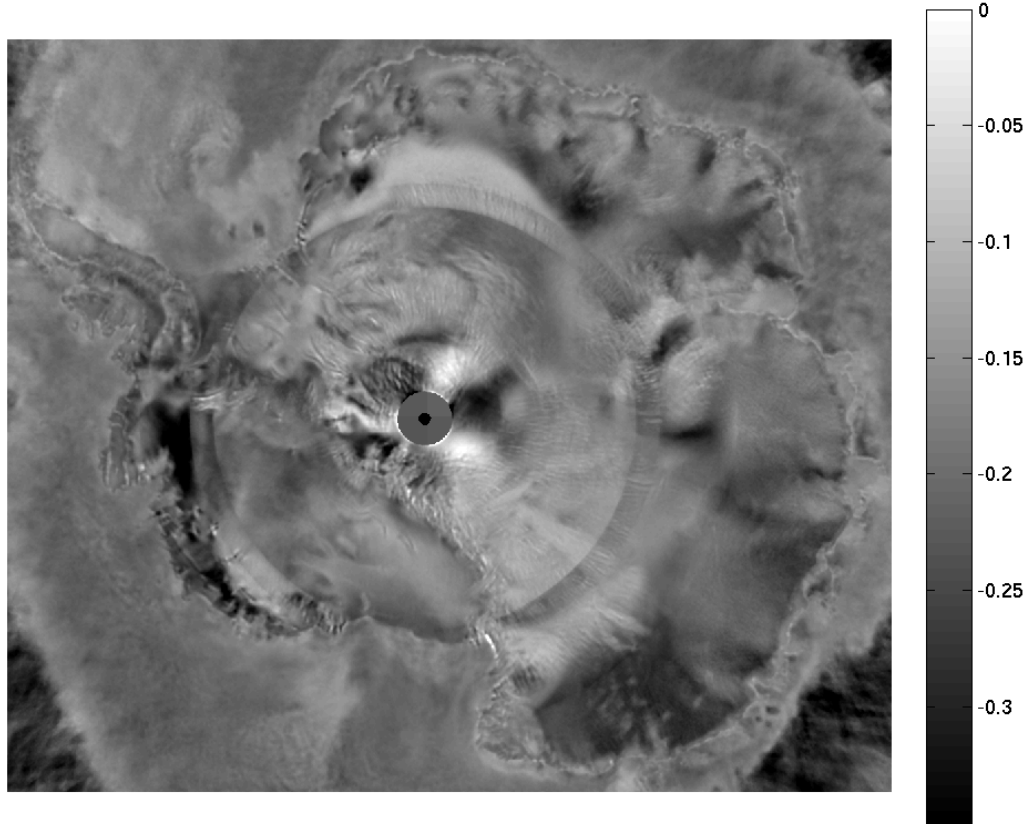


*Fig. A.2 ASCAT C-band slope of  $\sigma_0$  in dB/deg at a 40 degree incidence angle (termed 'b'). For latitudes less than approximately 78.25S, the distribution of measurements in incidence is altered since all the observations of a given point are limited to a single side of the spacecraft, resulting in a visible transition band and reduced accuracy near the pole. No estimates are possible for latitudes less than 88.5S due to lack of coverage.*

ASCAT H-pol q (1st Az Har) (msfa-q-Ant10-182-212.sir) in dB

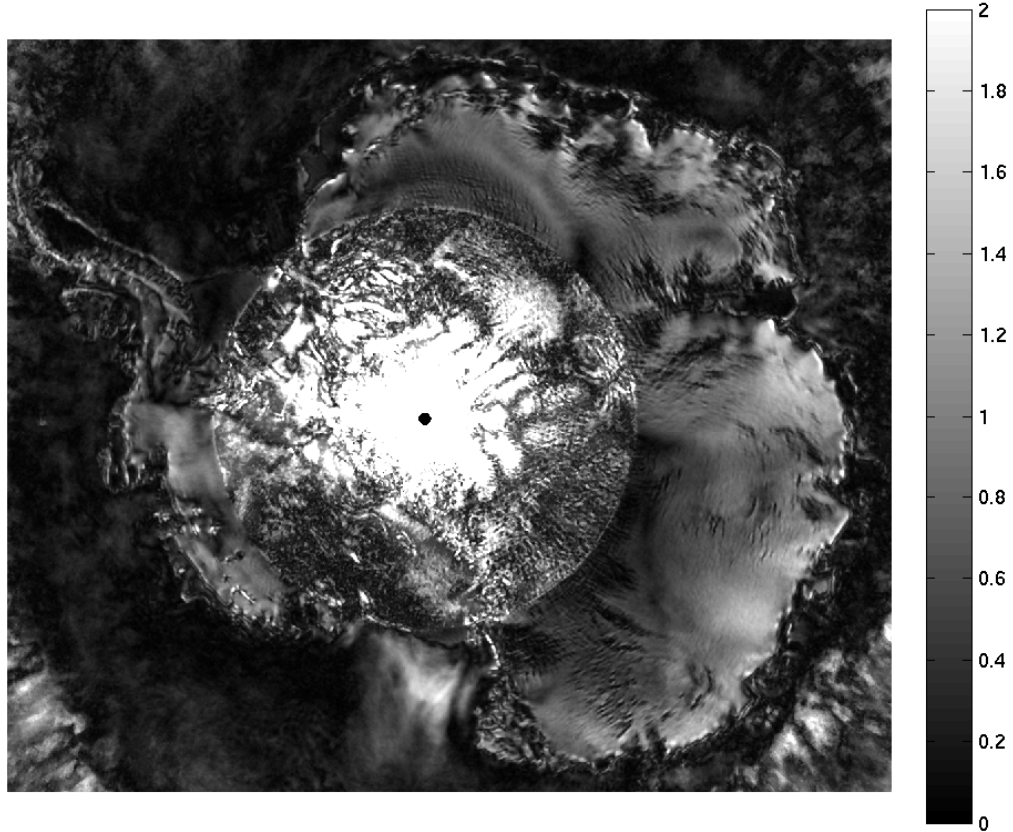


*Fig. A.3 ASCAT C-band first-order azimuth modulation magnitude parameter in dB (termed 'q'). Note that due to the ASCAT antenna beam and orbit geometry, the accuracy of parameters estimated for latitudes less than approximately 78.25S falls off.*

ASCAT H-pol r (1st Az Har phase) (msfa-q-Ant10-182-212.sir) in deg



*Fig. A.4 ASCAT C-band first-order azimuth modulation direction parameter in deg (termed 'r'). Note that due to the ASCAT antenna beam and orbit geometry, the accuracy of parameters estimated for latitudes less than approximately 78.25S falls off.*

ASCAT H-pol s (2nd Az Har) (msfa-s-Ant10-182-212.sir) in dB

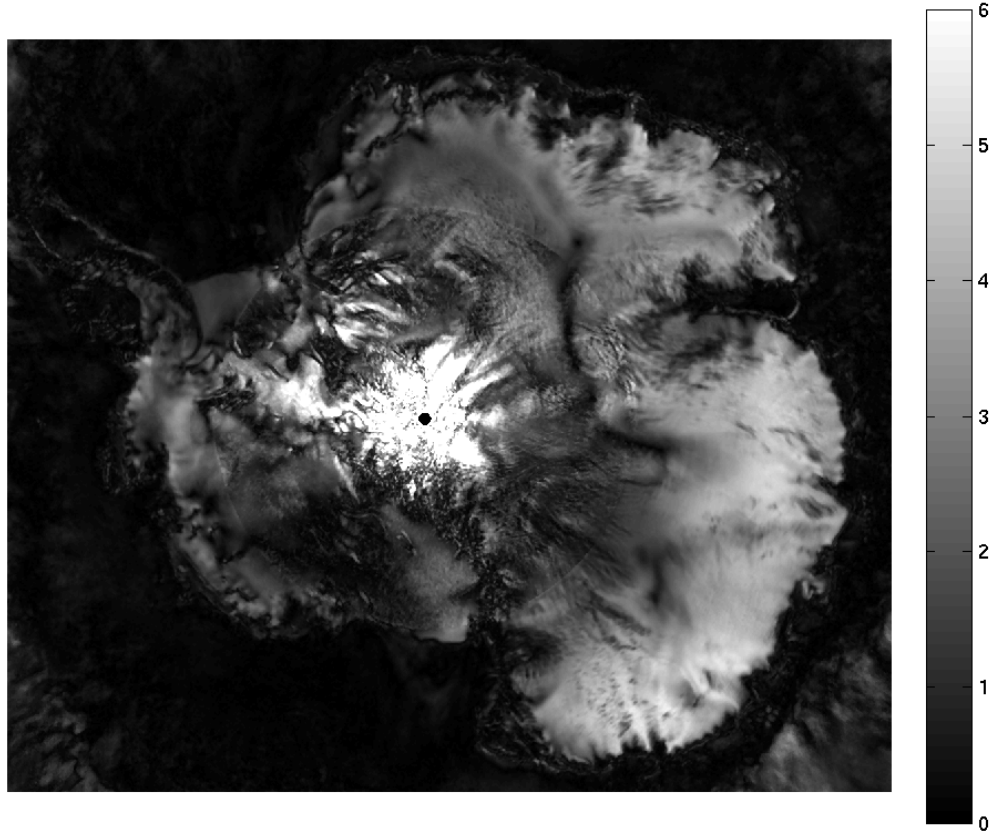


*Fig. A.5 ASCAT C-band second-order azimuth modulation magnitude parameter in dB (termed 's'). Note that due to the ASCAT antenna beam and orbit geometry, the accuracy of parameters estimated for latitudes less than approximately 78.25S falls off.*

ASCAT H-pol t (2nd Az Har phase) (msfa-t-Ant10-182-212.sir) in deg

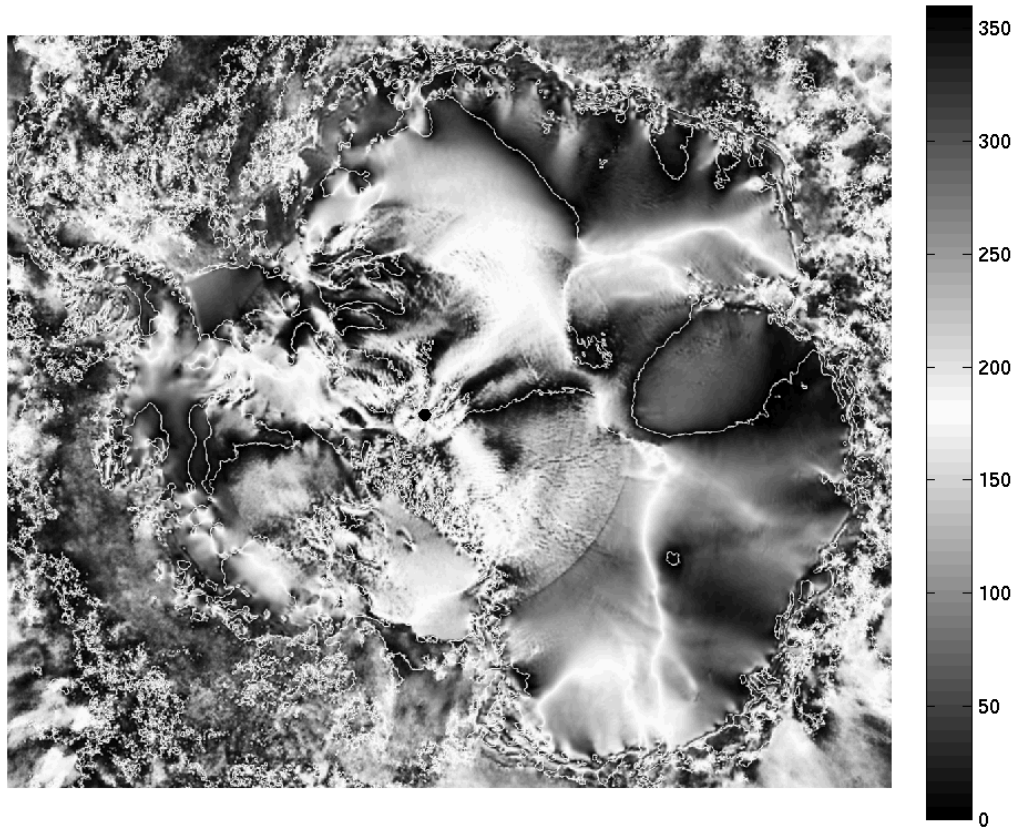


*Fig. A.6 ASCAT C-band second-order azimuth modulation direction parameter in deg (termed 't'). Note that due to the ASCAT antenna beam and orbit geometry, the accuracy of parameters estimated for latitudes less than approximately 78.25S falls off.*



ASCAT H-pol Q (3rd Az Har) (msfa-Q-Ant10-182-212.sir) in dB

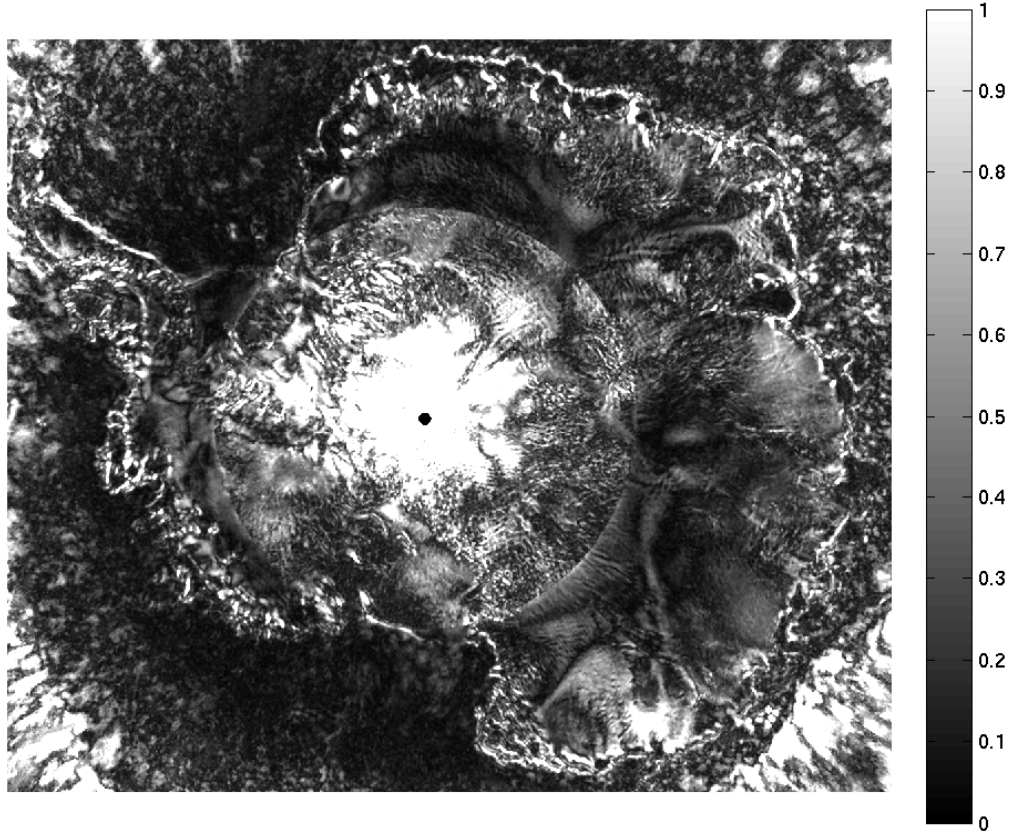


*Fig. A.7 ASCAT C-band third-order azimuth modulation magnitude parameter in dB (termed 'Q'). Note that due to the ASCAT antenna beam and orbit geometry, the accuracy of parameters estimated for latitudes less than approximately 78.25S falls off.*

ASCAT H-pol R (3rd Az Har phase) (msfa-R-Ant10-182-212.sir) in deg

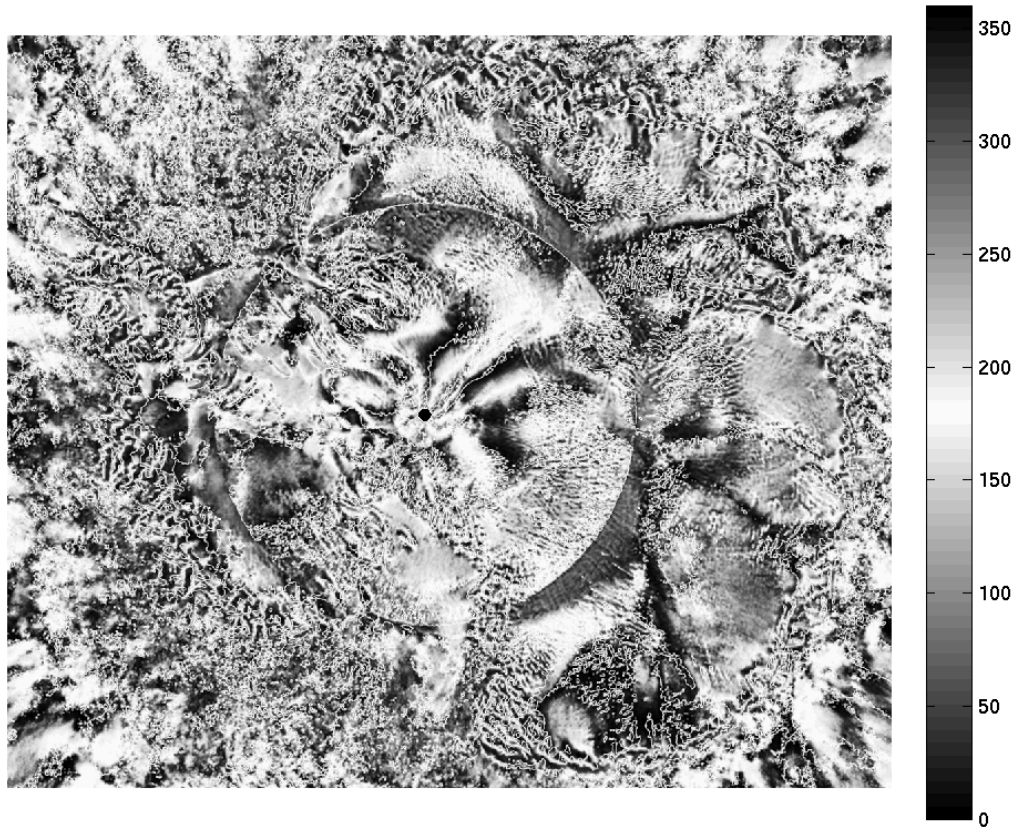


*Fig. A.8 ASCAT C-band third-order azimuth modulation direction parameter in deg (termed 'R'). Note that due to the ASCAT antenna beam and orbit geometry, the accuracy of parameters estimated for latitudes less than approximately 78.25S falls off.*

ASCAT H-pol S (4th Az Har) (msfa-S-Ant10-182-212.sir) in dB

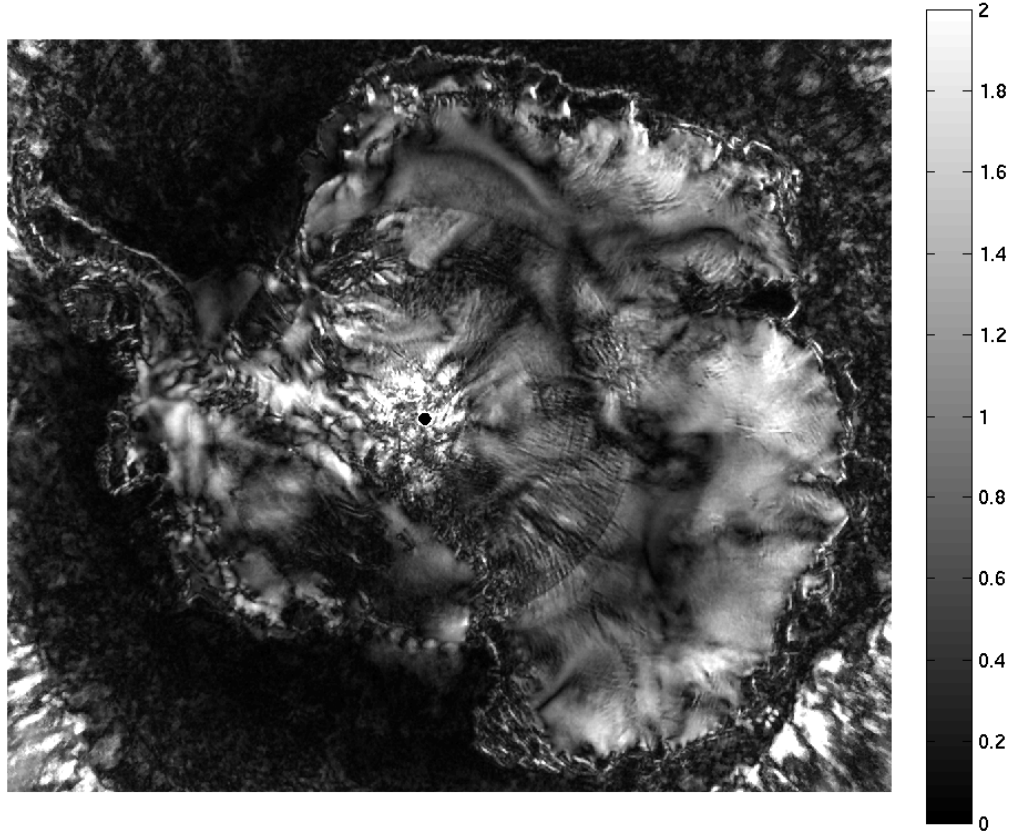


*Fig. A.9 ASCAT C-band fourth-order azimuth modulation magnitude parameter in dB (termed 'S'). Note that due to the ASCAT antenna beam and orbit geometry, the accuracy of parameters estimated for latitudes less than approximately 78.25S falls off.*

ASCAT H-pol T (4th Az Har phase) (msfa-T-Ant10-182-212.sir) deg

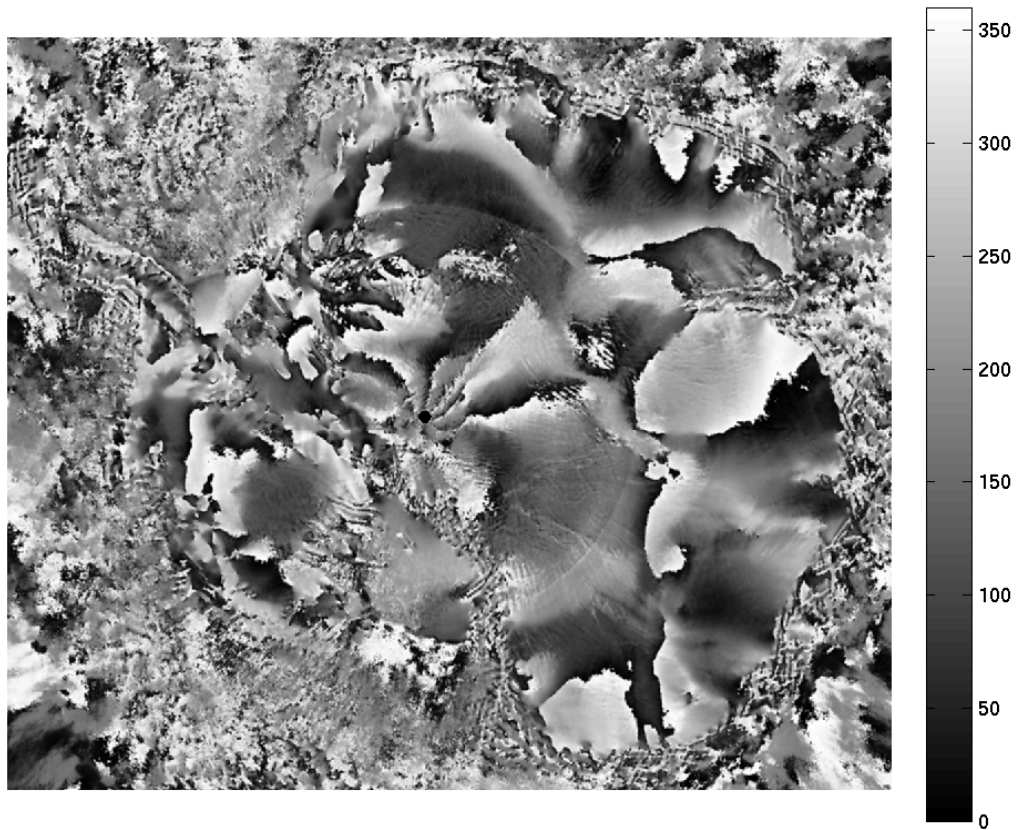


*Fig. A.10 ASCAT C-band fourth-order azimuth modulation direction parameter in deg (termed 'T'). Note that due to the ASCAT antenna beam and orbit geometry, the accuracy of parameters estimated for latitudes less than approximately 78.25S falls off.*

## Appendix B

This appendix illustrates the various coefficients of QuikSCAT (Ku-band) 4<sup>th</sup> order azimuth modulation dataset. The various terms in the model are described in Eq. 1 in the main text. Note that QuikSCAT is dual polarization where measurements are made at (essentially) a single incidence angle. Azimuth modulation images are computed separately for each polarization. Depending on latitude, the azimuth diversity at a given pixel varies. This degrades the azimuth modulation estimates near the pole. We are currently investigating methods for ameliorating this. Due to the method of estimating 'a' (mean sigma-0) first, 'a' image is not significantly affected by the reduced azimuth diversity.

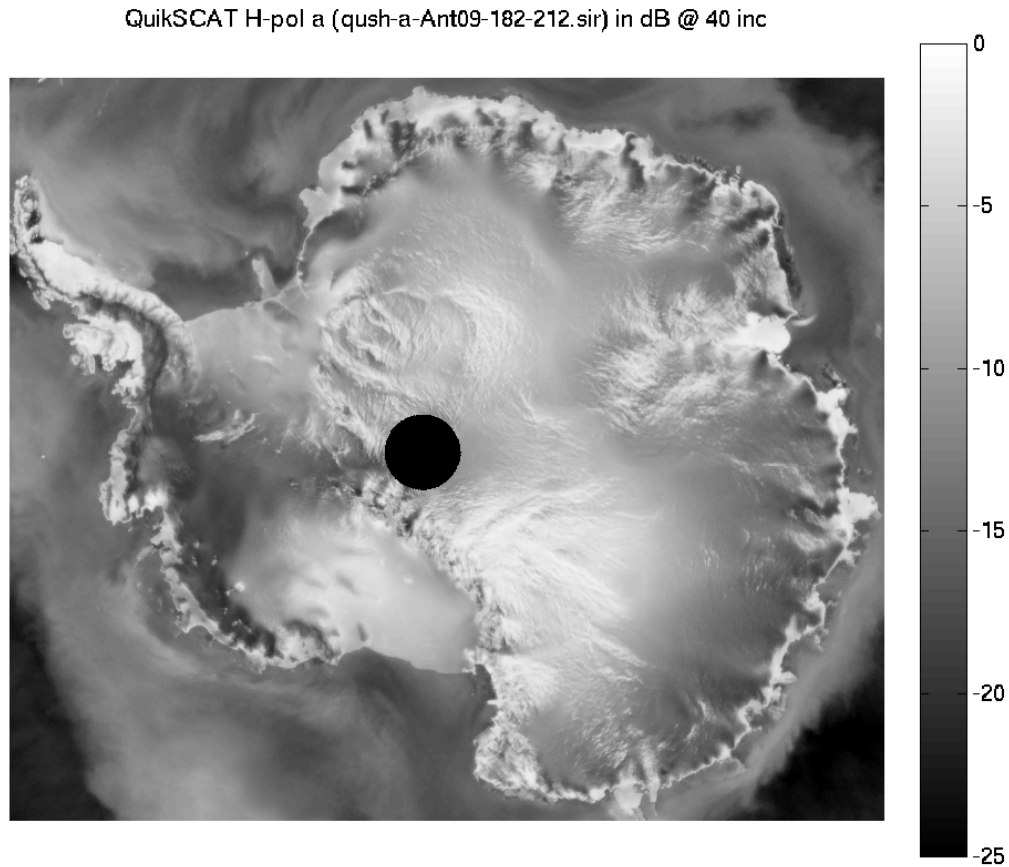


*Fig. B.1 QuikSCAT Ku-band H-pol sigma-0 in dB at a 46 degree incidence angle (termed 'a').*

QuikSCAT V-pol S (4th Az Har) (qusv-S-Ant09-182-212.sir) in dB

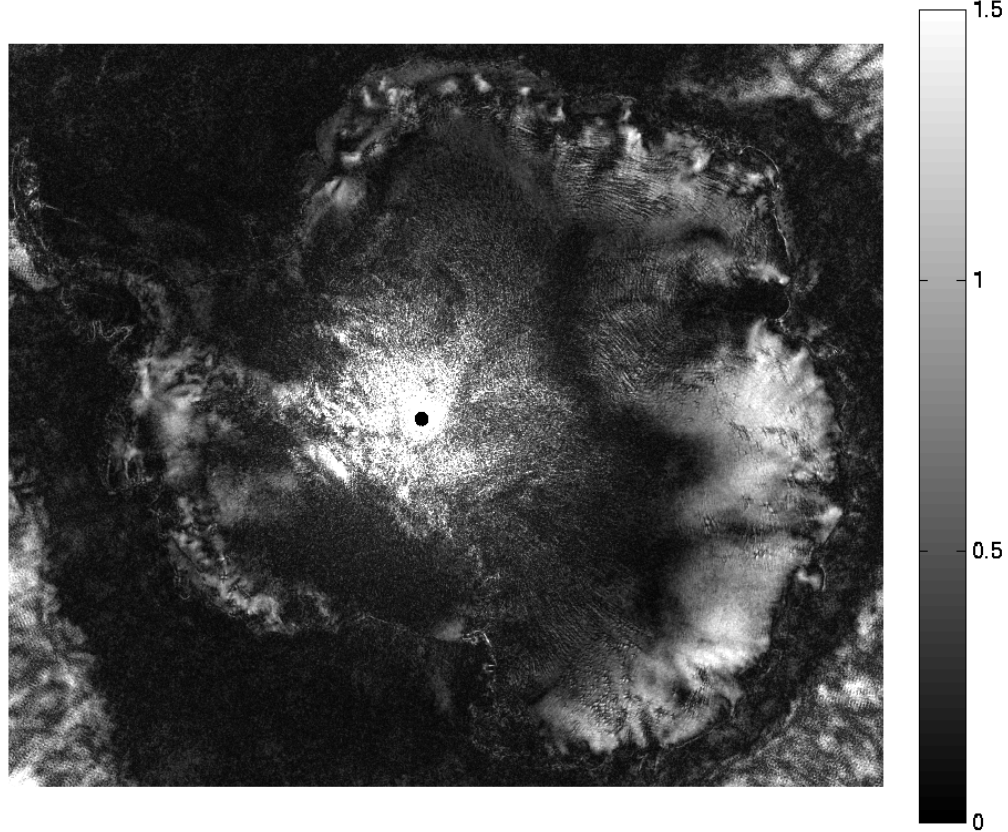


*Fig. B.2 QuikSCAT Ku -band H-pol first-order azimuth modulation magnitude parameter in dB (termed 'q'). Accuracy is reduced near the pole due to inadequate azimuth diversity.*

QuikSCAT H-pol  $r$  (1st Az Har phase) (qush-q-Ant09-182-212.sir) in deg

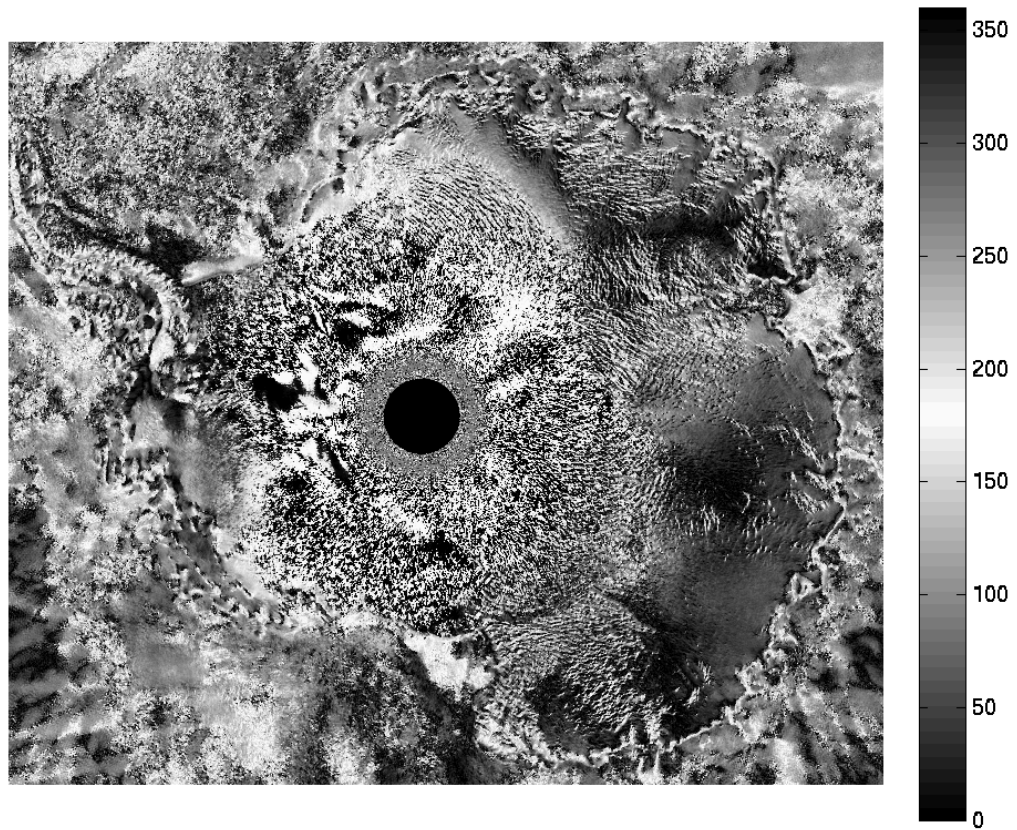


*Fig. B.3 QuikSCAT Ku -band H-pol first-order azimuth modulation direction parameter in deg (termed 'r'). Accuracy is reduced near the pole due to inadequate azimuth diversity.*

QuikSCAT V-pol  $s$  (2nd Az Har) (qusv-s-Ant09-182-212.sir) in dB

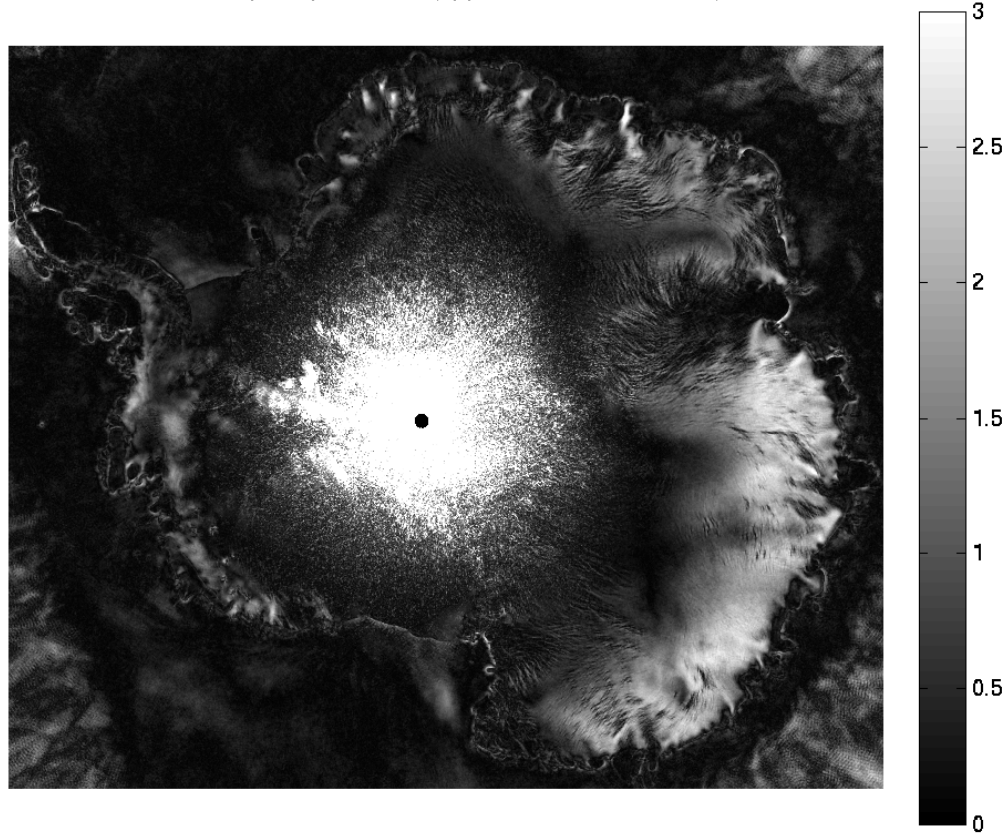


*Fig. B.4 QuikSCAT Ku -band H-pol second-order azimuth modulation magnitude parameter in dB (termed 's'). Accuracy is reduced near the pole due to inadequate azimuth diversity..*



QuikSCAT H-pol  $t$  (2nd Az Har phase) (qush-t-Ant09-182-212.sir) in deg

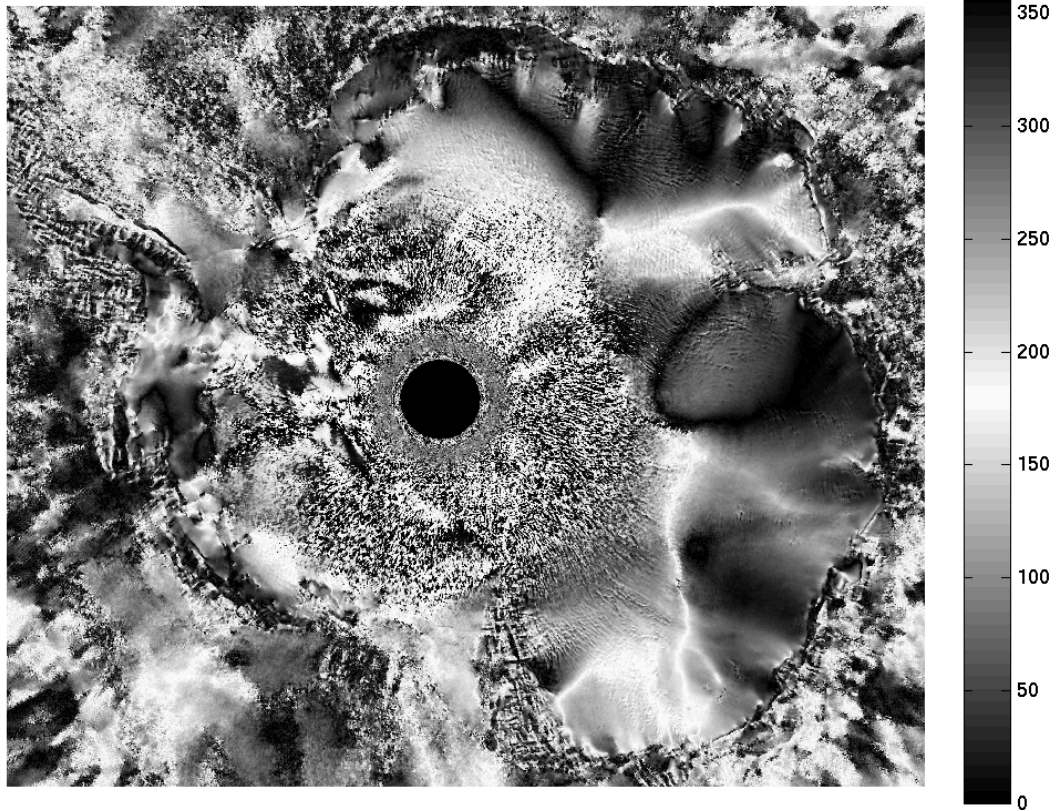


*Fig. B.5 QuikSCAT Ku -band H-pol second-order azimuth modulation direction parameter in deg (termed 't'). Accuracy is reduced near the pole due to inadequate azimuth diversity.*

QuikSCAT H-pol Q (3rd Az Har) (qush-Q-Ant09-182-212.sir) in dB

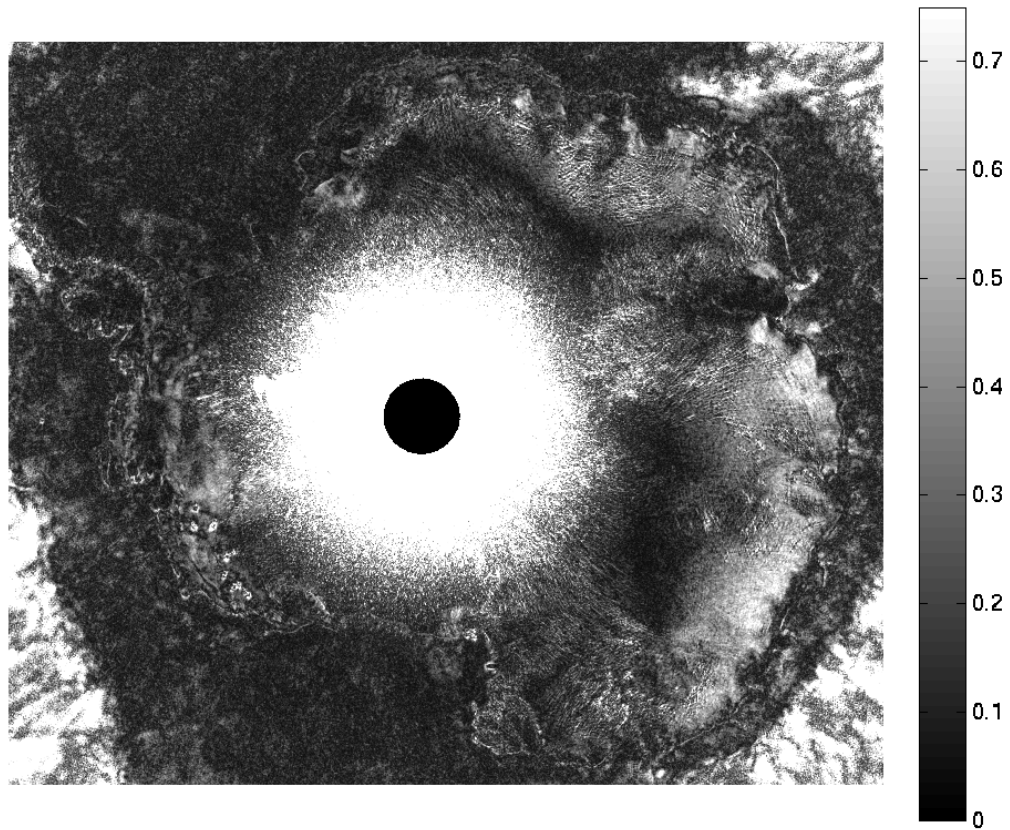


*Fig. B.6 QuikSCAT Ku -band H-pol third-order azimuth modulation magnitude parameter in dB (termed 'Q'). Accuracy is reduced near the pole due to inadequate azimuth diversity.*

QuikSCAT H-pol R (3rd Az Har phase) (qush-R-Ant09-182-212.sir) in deg

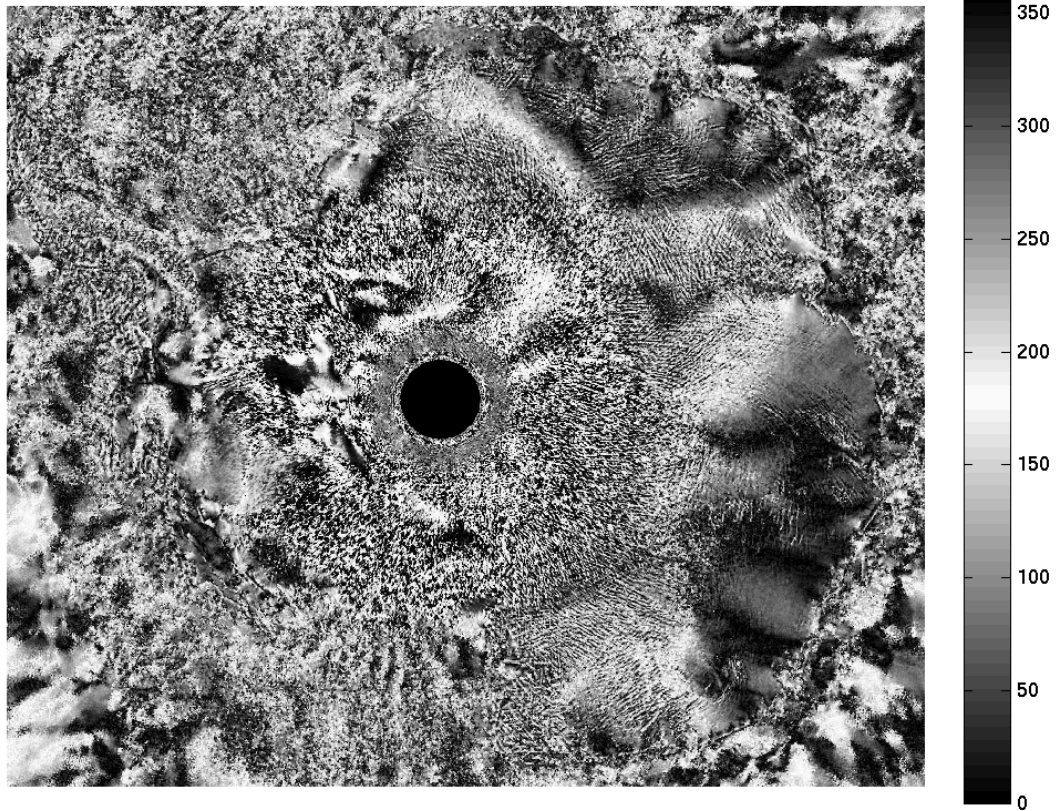


*Fig. B.7 QuikSCAT Ku -band H-pol third-order azimuth modulation direction parameter in deg (termed 'R'). Accuracy is reduced near the pole due to inadequate azimuth diversity.*

QuikSCAT H-pol S (4th Az Har) (qush-S-Ant09-182-212.sir) in dB

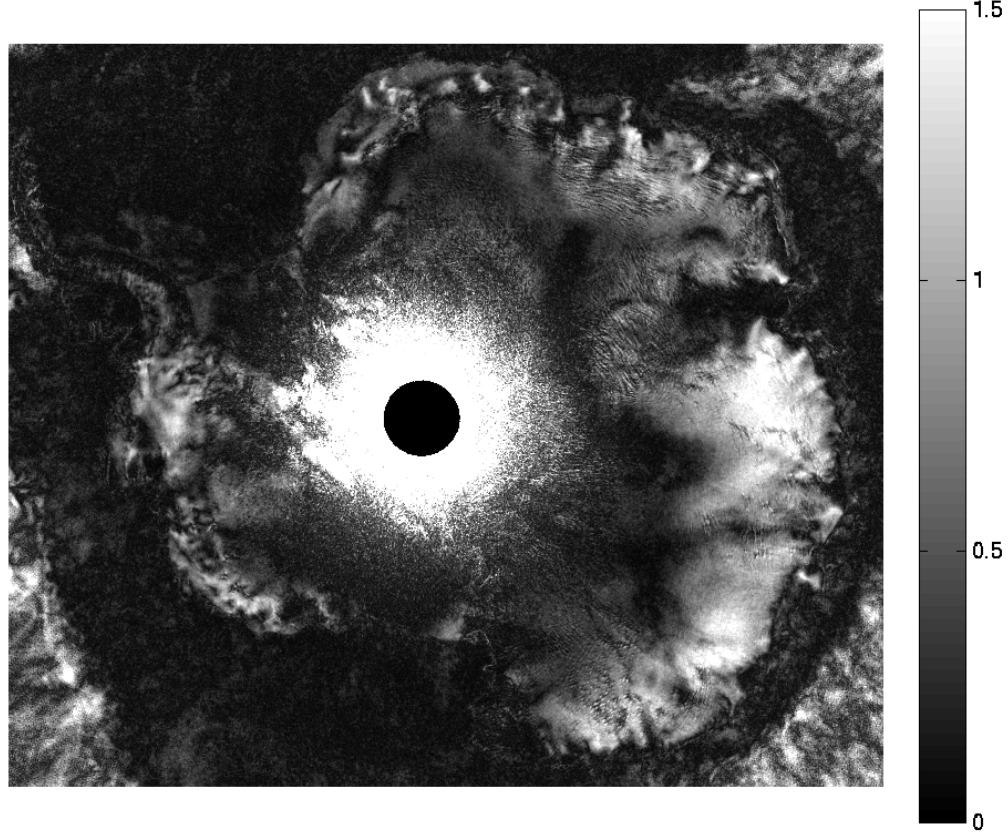


*Fig. B.8 QuikSCAT Ku -band H-pol fourth-order azimuth modulation magnitude parameter in dB (termed 'S'). Accuracy is reduced near the pole due to inadequate azimuth diversity.*

QuikSCAT V-pol s (2nd Az Har) (qusv-s-Ant09-182-212.sir) in dB

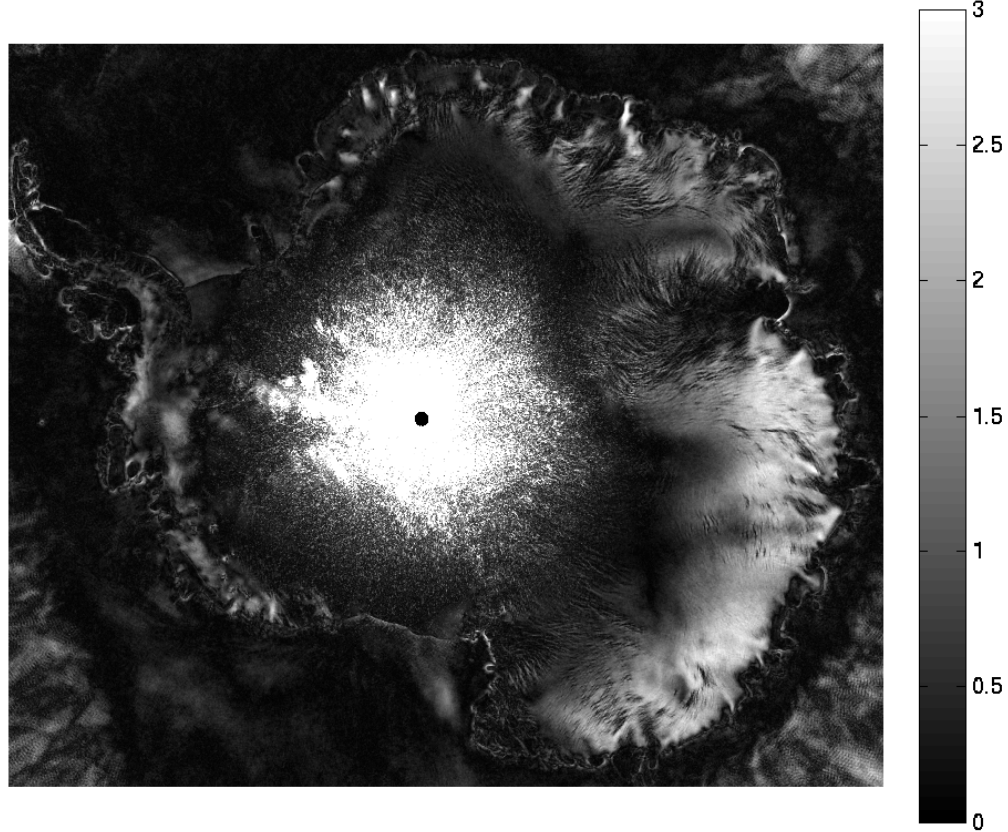


*Fig. B.9 QuikSCAT Ku -band H-pol fourth-order azimuth modulation direction parameter in deg (termed 'T'). Accuracy is reduced near the pole due to inadequate azimuth diversity.*

QuikSCAT V-pol a (qusv-a-Ant09-182-212.sir) in dB @ 40 inc

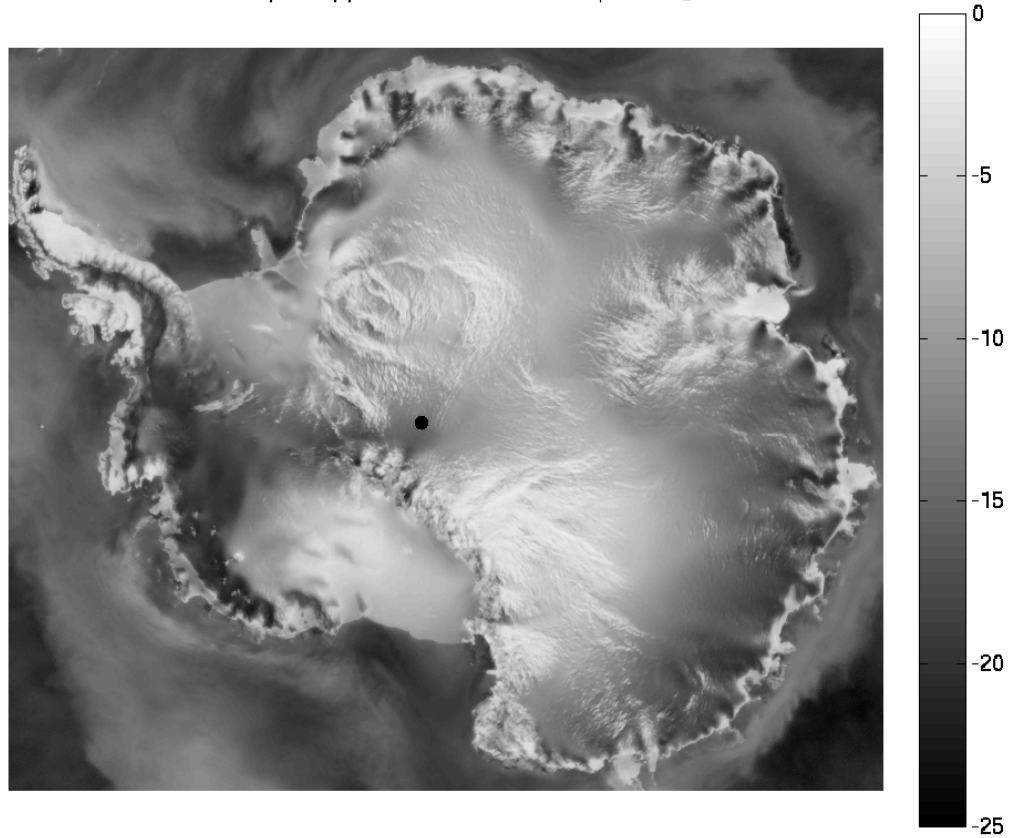


*Fig. B.10 QuikSCAT Ku -band V-pol sigma-0 in dB at a 56 degree incidence angle (termed 'a').*

QuikSCAT V-pol q (1st Az Har) (qusv-q-Ant09-182-212.sir) in dB

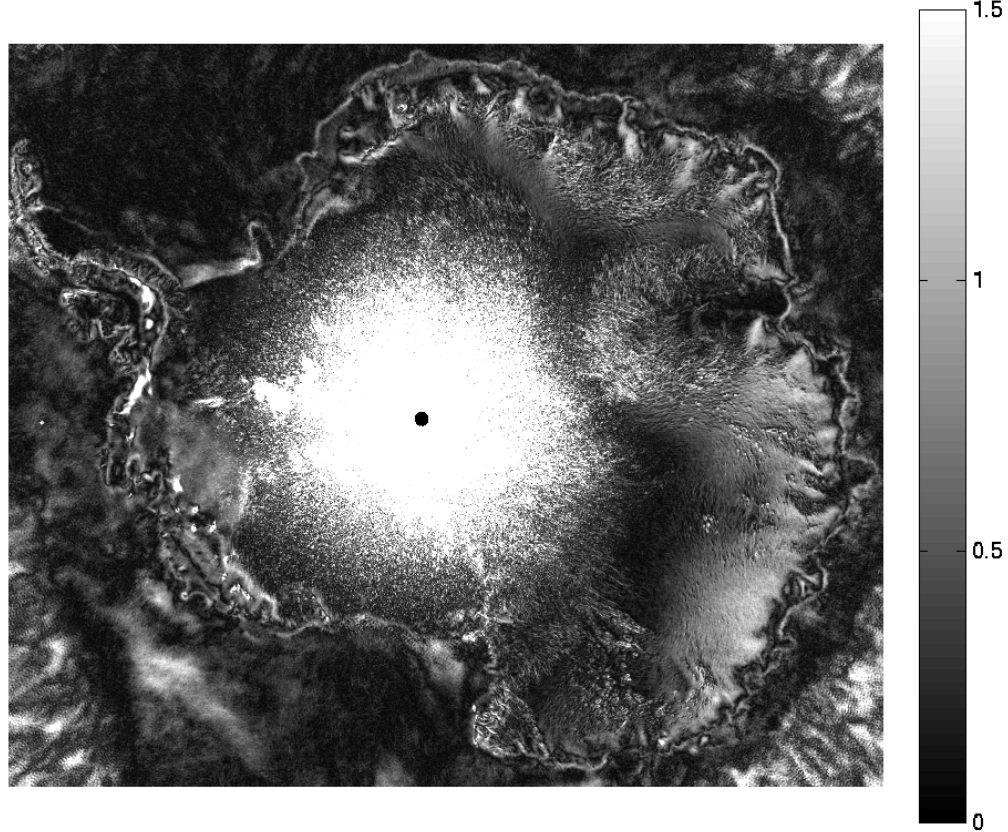


*Fig. B.11 QuikSCAT Ku -band V-pol first-order azimuth modulation magnitude parameter in dB (termed 'q'). Accuracy is reduced near the pole due to inadequate azimuth diversity.*

QuikSCAT V-pol r (1st Az Har phase) (qusv-q-Ant09-182-212.sir) in deg

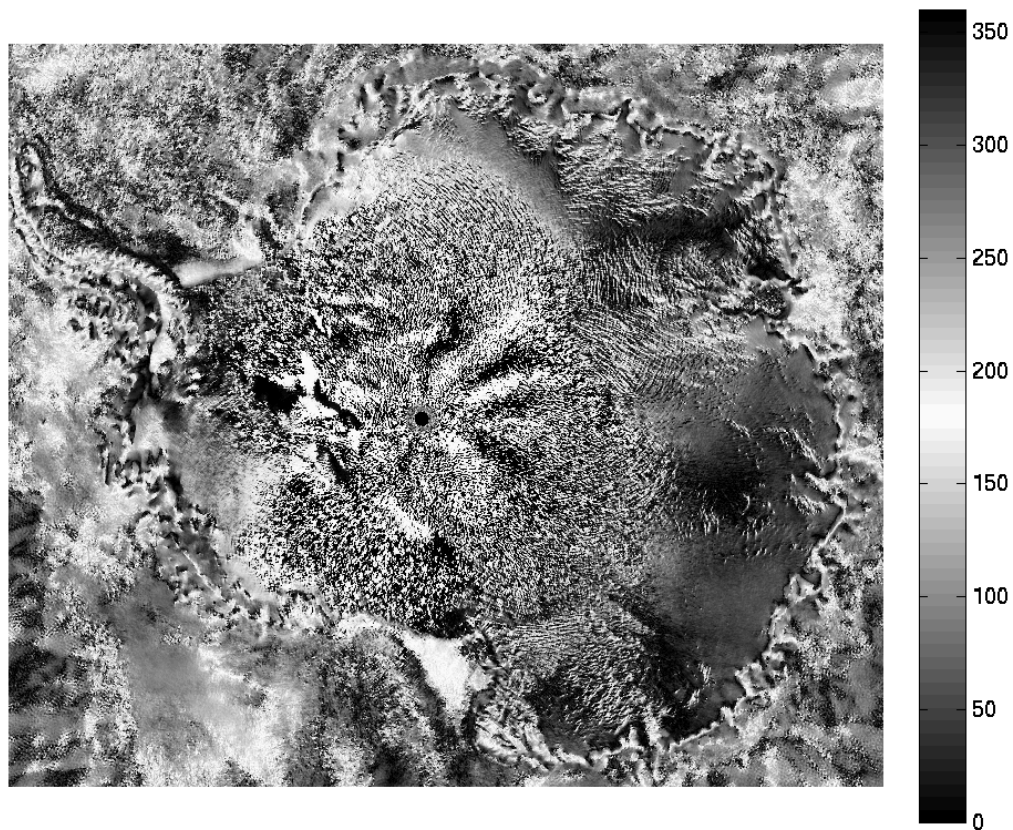


*Fig. B.12 QuikSCAT Ku -band V-pol first-order azimuth modulation direction parameter in deg (termed 'r'). Accuracy is reduced near the pole due to inadequate azimuth diversity.*



QuikSCAT V-pol s (2nd Az Har) (qusv-s-Ant09-182-212.sir) in dB

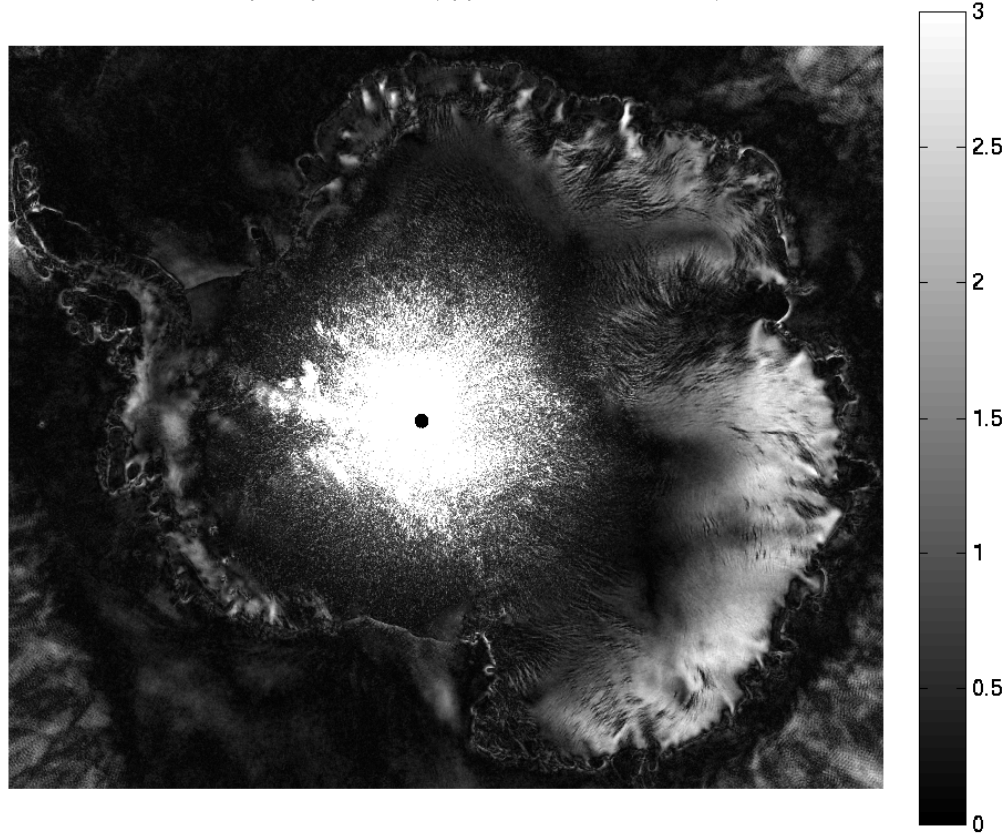


*Fig. B.13 QuikSCAT Ku -band V-pol second-order azimuth modulation magnitude parameter in dB (termed 's'). Accuracy is reduced near the pole due to inadequate azimuth diversity.*

QuikSCAT V-pol  $t$  (2nd Az Har phase) (qusv-t-Ant09-182-212.sir) in deg

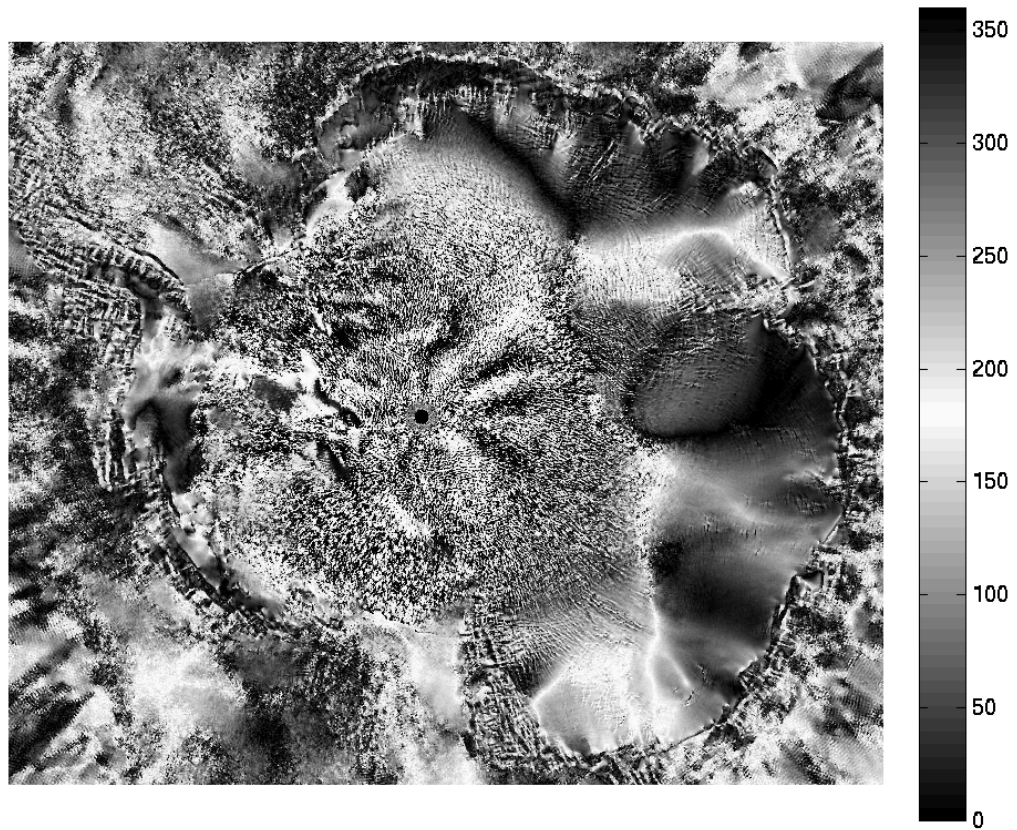


*Fig. B.14 QuikSCAT Ku -band V-pol second-order azimuth modulation direction parameter in deg (termed 't'). Accuracy is reduced near the pole due to inadequate azimuth diversity.*

QuikSCAT V-pol q (1st Az Har) (qusv-q-Ant09-182-212.sir) in dB

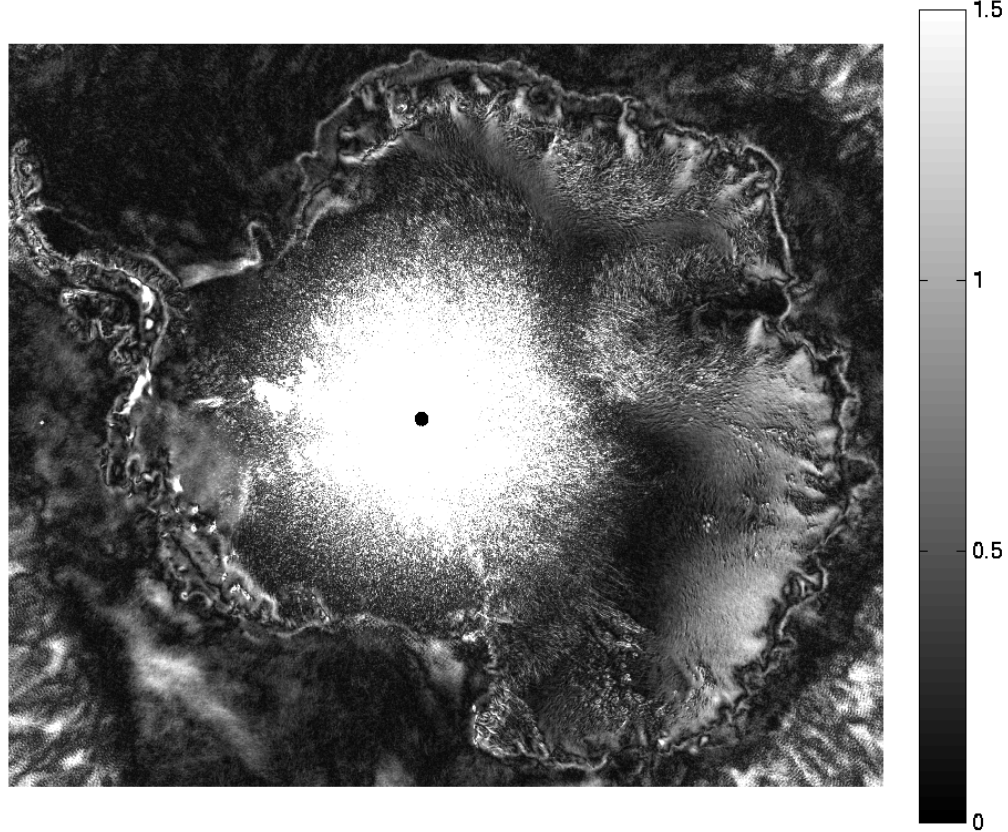


*Fig. B.15 QuikSCAT Ku -band V-pol third-order azimuth modulation magnitude parameter in dB (termed 'Q'). Accuracy is reduced near the pole due to inadequate azimuth diversity.*

QuikSCAT V-pol R (3rd Az Har phase) (qusv-R-Ant09-182-212.sir) in deg

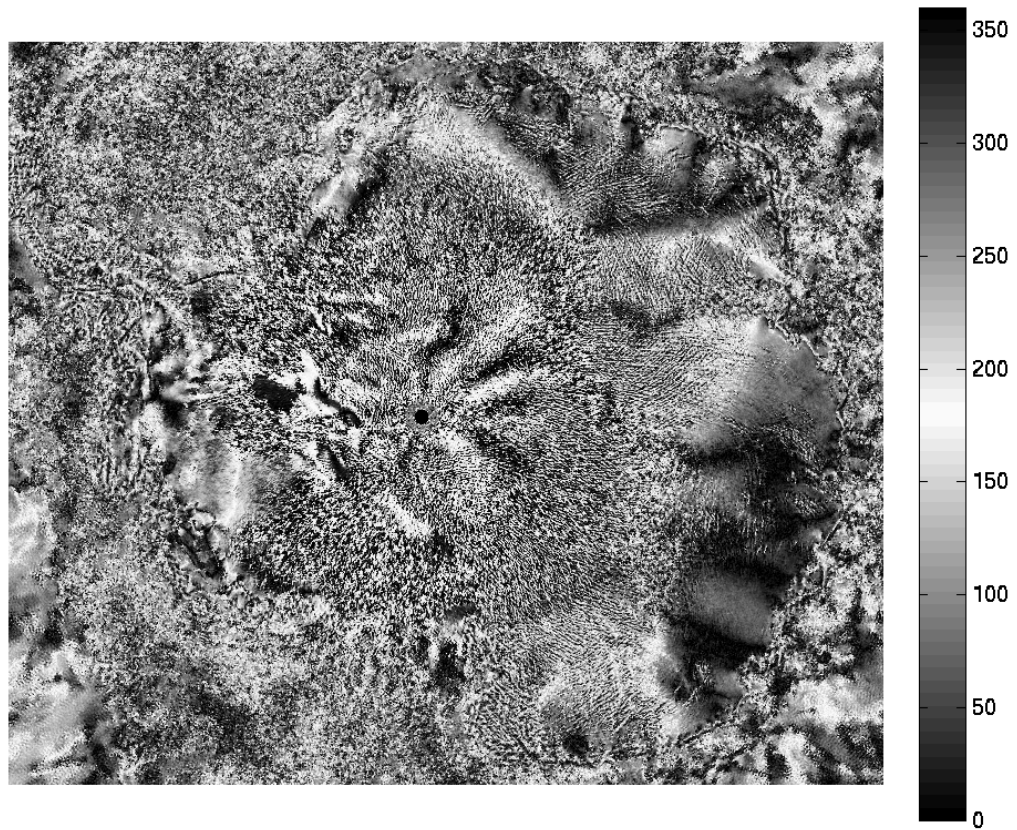


*Fig. B16 QuikSCAT Ku -band V-pol third-order azimuth modulation direction parameter in deg (termed 'R'). Accuracy is reduced near the pole due to inadequate azimuth diversity.*

QuikSCAT V-pol S (4th Az Har) (qusv-S-Ant09-182-212.sir) in dB

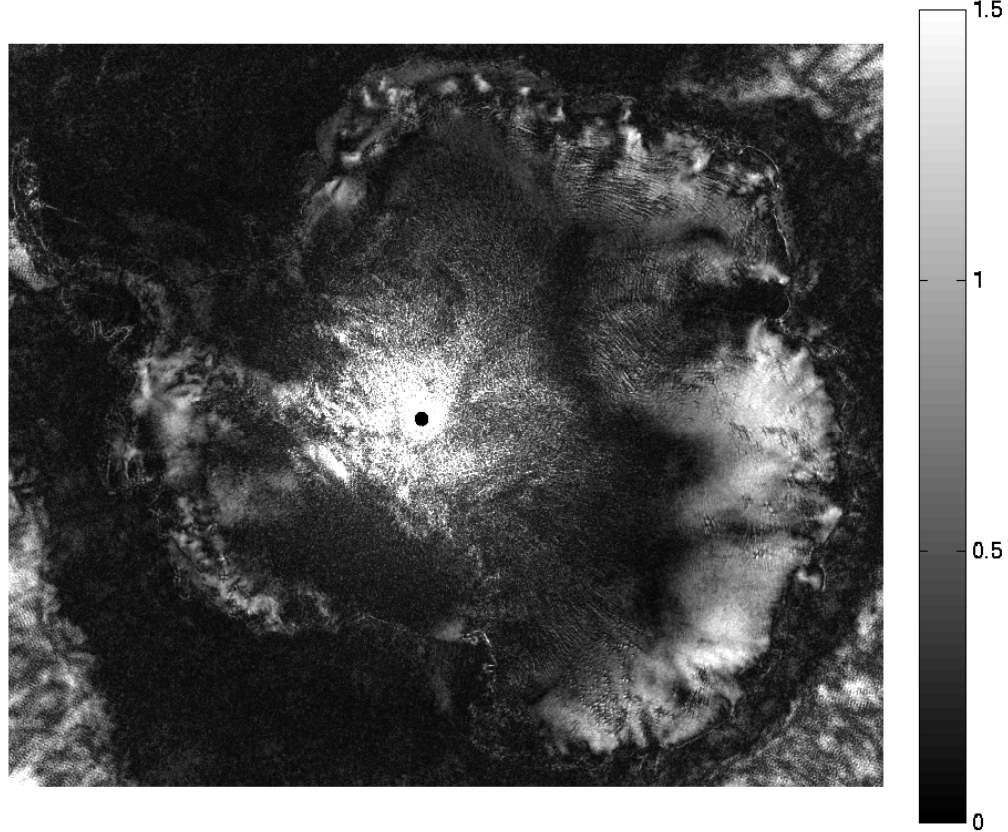


*Fig. B.17 QuikSCAT Ku -band V-pol fourth-order azimuth modulation magnitude parameter in dB (termed 'S'). Accuracy is reduced near the pole due to inadequate azimuth diversity.*

QuikSCAT V-pol S (4th Az Har) (qusv-S-Ant09-182-212.sir) in dB

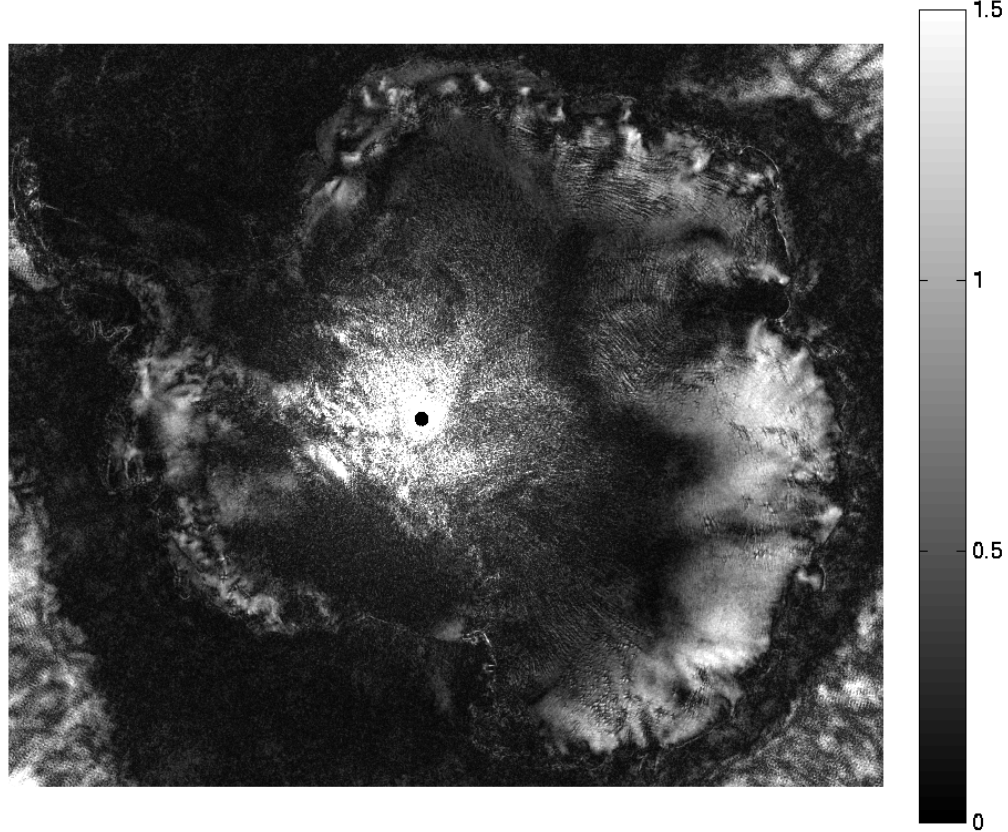


*Fig. B.18 QuikSCAT Ku -band V-pol fourth-order azimuth modulation direction parameter in deg (termed 'T'). Accuracy is reduced near the pole due to inadequate azimuth diversity.*